Nagra
Nationale
Genossenschaft
für die Lagerung
radioaktiver Abfälle

Cédra
Société coopérative
nationale
pour l'entreposage
de déchets radioactifs

Cisra
Società cooperativa
nazionale
per l'immagazzinamento
di scorie radioattive

TECHNICAL REPORT 88-32

CROSSHOLE INVESTIGATIONS – IMPLEMENTATION AND FRACTIONAL DIMENSION INTERPRETATION OF SINUSOIDAL TESTS

D. Noy
J. Barker
J. Black
D. Holmes

FEBRUARY 1988

BRITISH GEOLOGICAL SURVEY, United Kingdom

Parkstrasse 23 5401 Baden/Schweiz Telephon 056/20 55 11

Nagra
Nationale
Genossenschaft
für die Lagerung
radioaktiver Abfälle

Cédra
Société coopérative
nationale
pour l'entreposage
de déchets radioactifs

Cisra
Società cooperativa
nazionale
per l'immagazzinamento
di scorie radioattive

TECHNICAL REPORT 88-32

CROSSHOLE INVESTIGATIONS – IMPLEMENTATION AND FRACTIONAL DIMENSION INTERPRETATION OF SINUSOIDAL TESTS

D. Noy
J. Barker
J. Black
D. Holmes

FEBRUARY 1988

BRITISH GEOLOGICAL SURVEY, United Kingdom

Parkstrasse 23 5401 Baden/Schweiz Telephon 056/20 55 11

Der vorliegende Bericht betrifft eine Studie, die für das Stripa-Projekt ausgeführt wurde. Die Autoren haben ihre eigenen Ansichten und Schlussfolgerungen dargestellt. Diese müssen nicht unbedingt mit denjenigen des Auftraggebers übereinstimmen.

Le présent rapport a été préparé pour le projet de Stripa. Les opinions et conclusions présentées sont celles des auteurs et ne correspondent pas nécessairement à ceux du client.

This report concerns a study which was conducted for the Stripa Project. The conclusions and viewpoints presented in the report are those of the authors and do not necessarily coincide with those of the client.

Das Stripa-Projekt ist ein Projekt der Nuklearagentur der OECD. Unter internationaler Beteiligung werden von 1980-86 Forschungsarbeiten in einem unterirdischen Felslabor in Schweden durchgeführt. Diese sollen die Kenntnisse auf folgenden Gebieten erweitern:
- hydrogeologische und geochemische Messungen in Bohrlöchern
- Ausbreitung des Grundwassers und Transport von Radionukliden durch Klüfte im Gestein
- Verhalten von Materialien, welche zur Verfüllung und Versiegelung von Endlagern eingesetzt werden sollen
- Methoden zur zerstörungsfreien Ortung von Störzonen im Fels

Seitens der Schweiz beteiligt sich die Nagra an diesen Untersuchungen. Die technischen Berichte aus dem Stripa-Projekt erscheinen gleichzeitig in der NTB-Serie der Nagra.

The Stripa Project is organised as an autonomous project of the Nuclear Energy Agency of the OECD. In the period from 1980-86, an international cooperative programme of investigations is beeing carried out in an underground rock laboratory in Sweden. The aim of the work is to improve our knowledge in the following areas:
- hydrogeological and geochemical measurement methods in boreholes
- flow of groundwater and transport of radionuclides in fissured rock
- behaviour of backfilling and sealing materials in a real geological environment
- non-destructive methods for location of disturbed zones in the rock

Switzerland is represented in the Stripa Project by Nagra and the Stripa Project technical reports appear in the Nagra NTB series.

Le projet Stripa est un projet autonome de l'Agence de l'OCDE pour l'Energie Nucléaire. Il s'agit d'un programme de recherche avec participation internationale, qui sera réalisé entre 1980 et 1986 dans un laboratoire souterrain, en Suède. Le but de ces travaux est d'améliorer et d'étendre les connaissances dans les domaines suivants:
- mesures hydrogéologiques et géochimiques dans les puits de forage
- chimie des eaux souterraines à grande profondeur
- écoulement des eaux souterraines et transport des radionucléides dans les roches fracturées
- comportement des matériaux de colmatage et de scellement des dépôts finals
- méthodes de localisation non destructive des zones de perturbation de la roche

La Suisse est représentée dans le projet Stripa par la Cédra. Les rapports techniques du projet Stripa sont publiés dans la série des rapports techniques de la Cédra (NTB).

ABSTRACT

The Crosshole Programme was an integrated geophysical and hydrogeological study of a limited volume of rock (known as the Crosshole Site) within the Stripa Mine. Borehole radar, borehole seismic and hydraulic methods were developed for specific application to fractured crystalline rock.

The hydrogeological investigations contained both single borehole and crosshole test techniques. A novel technique, using a sinusoidal variation of pressure, formed the main method of crosshole testing and was assessed during the programme. The strategy of crosshole testing was strongly influenced by the results from the geophysical measurements.

The crosshole sinusoidal testing was carried out using computer-controlled test equipment to generate the sinusoidally varying head in a single zone (the "source") isolated by packers. A second ("receiver") borehole contained a number of straddle intervals and was used to observe the propagation of the sinusoidal signal. The number of positive responses was limited and flow appeared to be concentrated within a few "channels". Analysis was attempted using single fissure, regularly fissured and porous medium models. None gave satisfactory fits to the measured data. A new analysis involving the "dimension" of the flow test has been developed to analyse the results of the crosshole sinusoidal testing. This analysis allows the dimension of the flow to assume non-integer values whereas conventionally the dimension is taken as either one, two, or three: for example, radial flow in a uniform planar fissure would be two dimensional.

The new model is found to give a more consistent description of the test data than the conventional models and suggests a complex pattern of fracture properties within each fracture zone. However, the results presented must be considered as being preliminary since we still have much to learn about how to best apply this model and present the results. Also, it is not yet clear how the derived value of "dimension" can be related to the transport properties of the rock.

RESUME

Le programme "Crosshole" (entre forages) représentait une étude géophysique et hydrogéologique intégrée d'un volume rocheux limité (ledit site "Crosshole") dans la mine de Stripa. Des méthodes d'investigation spécifiques pour l'étude de roches cristallines fracturées furent développées: radar en forage, sismique en forage et essais hydrauliques.

Les investigations hydrogéologiques consistaient en techniques d'essais dans un forage unique ainsi qu'entre forages. Une nouvelle technique utilisant une variation sinusoïdale de la pression représentait la méthode principale de ce programme d'essais entre forages lors duquel elle fut évaluée. La stratégie des essais entre forages a été fortement influencée par les résultats des mesures géophysiques.

Les essais sinusoïdaux entre forages ont été réalisés en utilisant un équipement piloté par ordinateur pour générer la pression variant sinusoïdalement dans une zone unique isolée par des packers (la "source"). Un second forage ("récepteur"), subdivisé en un certain nombre d'intervalles, servait à l'observation de la propagation du signal sinusoïdal. Le nombre de réponses positives fut limité et les écoulements semblaient se concentrer dans quelques "canaux" seulement. On tenta d'élaborer une analyse par des modèles représentant une seule fissure, des milieux régulièrement fissurés et des milieux poreux. Aucun d'eux n'a donné de correspondance satisfaisante avec les valeurs mesurées. Une nouvelle analyse intégrant la "dimension" de l'essai de circulation a été développée pour analyser les résultats des essais sinusoïdaux entre forages. Cette analyse permet d'attribuer à la circulation une dimension de valeur non entière alors que conventionellement la dimension prend la valeur un, deux ou trois; ainsi par exemple un écoulement radial dans une fissure plane uniforme serait à deux dimensions.

Le nouveau modèle s'avère donner une description plus compatible avec les résultats des mesures que la méthode conventionnelle et suggère une image complexe des propriétés des fractures à l'intérieur de chaque zone de fracture. Les résultats présentés doivent toutefois être considérés comme préliminaires car nous avons encore beaucoup à apprendre sur la façon d'appliquer au mieux ce modèle et de présenter les résultats. Il n'est par aillleurs pas encore clair comment la valeur dérivée pour la "dimension" peut être liée aux caractéristiques de transport de la roche.

ZUSAMMENFASSUNG

Unter der Bezeichnung Crosshole-Programm wurde eine integrierte geophysikalische und hydrogeologische Untersuchung des Gesteins durchgeführt, in einem räumlich begrenzten Bereich des Stripa-Bergwerks, der Crosshole-Standort genannt wird. Dabei wurden Bohrlochradar sowie seismische und hydraulische Bohrlochmessmethoden für spezielle Anwendungen im geklüfteten Kristallin entwickelt.

Hydrogeologische Untersuchungen umfassten sowohl Messungen aus einem Bohrloch als auch Crosshole-Tests. Eine neue Messmethode, bei der der Druckverlauf sinusförmig variiert wird, bildete den wichtigsten Bestandteil der Crosshole-Messungen. Die Möglichkeiten und Grenzen dieser Methode konnten bei den Untersuchungen abgeklärt werden. Die Untersuchungsstrategie bei den Crosshole-Tests wurde stark beeinflusst durch die Ergebnisse der geophysikalischen Messungen.

Beim Sinus-Crosshole-Test wurde mit Hilfe einer rechnergestützten Versuchseinrichtung in einem einzigen, durch Packer abgetrennten Bohrlochbereich ("Quelle") der Druck sinusförmig variiert. Ein zweites Bohrloch ("Empfänger") mit einer Anzahl von abgepackerten Messintervallen wurde zur Beobachtung der Ausbreitung des Sinus-Signals benutzt. Auswertbare Ergebnisse konnten nur in wenigen Intervallen erhalten werden - der Wasserfluss scheint auf einige wenige "Kanäle" konzentriert zu sein. Es wurde vergeblich versucht, die Messergebnisse mit Hilfe von Standardmodellen (einzelne Kluft, gleichmässige Klüftung, poröses Medium) rechnerisch darzustellen - keines der Modelle beschrieb aber die experimentell ermittelte Situation zufriedenstellend. Zur Analyse der Messresultate wurde deshalb eine neue Modellierungs-Methode entwickelt, bei der die "Dimension" des Fliess-Systems beliebig gewählt werden kann, im Gegensatz zu den konventionellen Modellen, in denen nur ganzzahlige Werte 1, 2 oder 3 zugelassen sind (als Beispiel mag radialer Fluss in einer planaren Kluft dienen, der die Dimension 2 hätte).

Das neue Modell beschreibt die gemessenen Werte mit weniger Widersprüchen als die konventionellen Fliessmodelle. Die Strömung lässt sich als das Resultat eines komplexen Musters der Klufteigenschaften innerhalb der einzelnen Störungszonen verstehen. Die hier dargestellten Ergebnisse müssen allerdings als vorläufig verstanden werden - es bestehen immer noch viele offene Fragen in Bezug auf die Anwendung des Modells und die Darstellung der Rechenergebnisse. Ausserdem ist noch nicht klar, wie der abgeleitete Wert der "Dimension" mit den Transporteigenschaften des Gesteins korreliert werden kann.

TABLE OF CONTENTS

LIST OF FIGURES

SUMMARY

The hydraulics programme of the Crosshole Project had roughly two aims, to "calibrate" the geophysical methods and to evaluate sinusoidal testing. The calibration of the geophysical methods is described in another report (Olsson and others, 1987).

The programme consisted of

1) the development of a novel set of test equipment
2) a series of crosshole sinusoidal tests
4) the development of a novel test interpretation for fractured rocks (fractional dimensions)
5) the application and interpretation of the fractional dimension test analysis

The programme showed that it is possible to design and construct a complex set of computer-controlled equipment and operate it regularly in the mine environment. The innovative aspects of the equipment were the use of a computer for test operation. This resulted in good quality data with a high resolution and a close adherence to the analytical assumptions underlying the test.

The sinusoidal testing had attributes which were not expected. Firstly it proved very easy to create a sinusoidal fluctuation since it requires neither rapid changes of flow rate or head or long periods of steady conditions. The computer produced sinusoidal fluctuations which were ideal. The main unexpected aspect of sinusoidal testing is its sensitivity to the correct assumption concerning the geometry of flow during a test.

The analysis of the sinusoidal tests resulted in a new analysis having to be adopted. In order to consistently interpret both source and receiver signals in these crosshole sinusoidal tests in fractured granite the concept of a fractional-dimension fracture system has been developed. This allows the treatment of channels, fissures,and homogeeously fractured rock as special cases of a continuous spectrum of flow concepts.

Results from long and short period tests need to be interpreted separately. It may be suggested that this is due the presence of different sizes of features in the fracture system. Thus small scale features dominate the short period responses whilst larger features determin the response to longer period input signals.

Fracture system conductivities measured by long period signals in zone A range from 1.9×10^{-5} to 1.0×10^{-4} m/s., whilst in zone C values of 5.9×10^{-5} and 5.8×10^{-4} were found. The dimensionality of zone C was found to be lower at larger distances than zone A, suggesting that it might be a thinner zone or possibly just less interaction between the channels. The interpretation of the short period data from zone A between boreholes 3 and 5 in terms of a 2.5D geometry also suggests that this zone is "thick" by comparison with a 12 min. period wave in this region.

The development of the fractional dimension analysis represents a first step towards flow concepts which have a universal application. It seems possible that it represents a practical method for deriving general hydraulic properties of channelled fracture zones. In general it is clear that the fractional dimension approach requires further investigation.

The bulk of the rock does not take part in regional flow. Instead it is concentrated to particularly active channels contained loosely within fracture zones. Of the two zones investigated by the crosshole sinusoidal method, Zone A appears to have a larger dimension than Zone C. This may indicate that Zone C is a sparser network of channels than Zone A.

A major result of the Crosshole Hydraulic Programme has been the necessity to re-examine many hydrogeological preconceptions.

1 INTRODUCTION

1.1 GENERAL BACKGROUND

The Crosshole Programme of Phase II of the Stripa Project has as a general objective the development of non-destructive site-characterisation methods for potential radioactive waste repositories. More particularly, the programme consists of using three separate techniques (radar, seismic and hydraulic) in the same volume of rock at the Stripa Mine in central Sweden. The intention was to compare the results and assess how well the remote sensing methods (seismic and radar) could be used to predict the groundwater flowpaths.

During the years 1983-1986 these three techniques have been deployed within the six boreholes which make up the "fan-array" of the Crosshole Site. There are therefore three almost separate pieces of work consisting of:

- radar investigations
- seismic investigations
- hydraulic (meaning physical hydrogeology) investigations

In addition to these applications of particular techniques there has also been a preliminary phase of site description (Carlsten and others, 1985) and a detailed description of the cores from the six boreholes (Carlsten and Stråhle, 1985). However, the three investigation techniques form the core of the programme and are reported separately as well as together.

The hydraulic investigations comprised two phases, a first phase of standard single borehole tests and a second phase of novel "sinusoidal" crosshole tests. An additional novel feature of the hydraulic investigations was the use of computer-controlled testing equipment designed to minimise errors and improve test control. These novel aspects are reported separately. Hence the equipment is described by Holmes (1984) and by Holmes and Sehlstedt (1987). An outline of the approach to be used for the interpretation of sinusoidal pressure tests was described by Black and others (1986). That report was written before the actual results had become available. In this report therefore, it is intended to describe the work that has been carried out, outline the results and interpret them in terms of the physical hydrogeology of the Crosshole Site.

After initial attempts at interpretation of the results it became clear that the interpretation theory previously put forward in Black and others (1986) was incomplete. This report is a description of the interpretation of the results of crosshole sinusoidal testing carried out within the Crosshole Project. The results and conclusions from this report are summarised in terms of the physical hydrogeology of the Crosshole Site in Black and others (1987).

There were two novel aspects concerning the hydraulic testing carried out in the Crosshole Project. The first was the use of the "sinusoidal" test technique and the second the use of computer controlled equipment to generate the test (rather than simply monitor the results).

The sinusoidal pressure test is a crosshole technique in which a small zone of one borehole is subjected to a sinusoidal variation of pressure whilst similar zones in adjacent boreholes are monitored (Figure 1.1a). The pressure variation in the source zone is created by a carefully controlled regime of injection and abstraction. The receiver zones should detect sinusoidally varying pressure which has a smaller amplitude than that in the source zone. Also the observed signal should lag behind the source zone signal since the pressure waves take some time to diffuse from the source to the receiver (Figure 1.1b). The decrease in amplitude and the retardation of the received signal depend on the geometry and hydrogeological properties of the flow paths in the vicinity of the source zone.

This approach has several advantages and disadvantages when compared to the usual constant-flow aquifer test, namely:

Advantages:

1. The oscillating signal (of known frequency) is detectable against a changing background pressure (especially important in mines).
2. The testing is essentially point to point enabling complex flow geometry to be built up from simpler smaller elements.
3. There is no net discharge so equilibration times are small, enabling rapid movements of the source zone position.
4. The frequency of the test is specific and can be changed to investigate different components of the bulk rock hydrogeology, i.e. fracture properties and matrix properties.

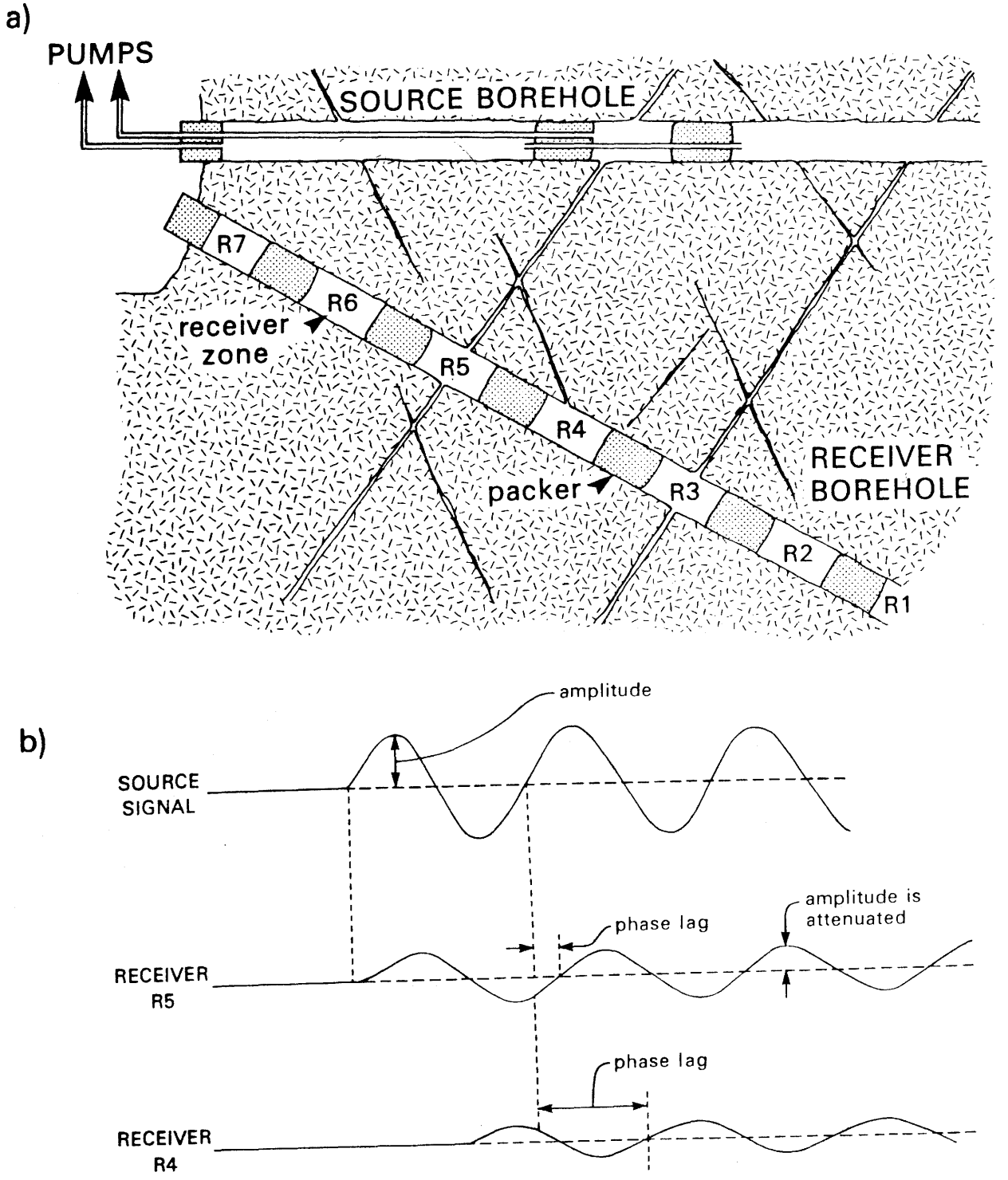

Figure 1.1 Schematic representation of a) source and receiver borehole arrangement
b) amplitude attenuation and phase lag

Disadvantages:

1. The distance of penetration of measurable pressure fluctuations is less than in the constant-flow method.
2. The test requires equipment which is more complicated than straightforward abstraction testing.

The test was first proposed by Black and Kipp, (1981) for a limited range of flow geometries. This was later extended to fissured rock in particular by Black and others, (1986). In the meantime some field experiments using slightly distorted manually-produced sinusoids had been carried out (Black and others, 1985). The experimental situation in the Crosshole Project seemed ideal for the first serious application of sinusoidal tests since the test distances were limited, the mine environment fluctuated generally and the properties of the fractures were of special importance.

1.2 NEW EQUIPMENT

The decision to use sinusoidal tests as the main method of crosshole testing resulted in the need for a set of testing equipment which could create sinusoidal variations of head in a source zone. Previously this had been done manually (Black and others, 1985) but this was obviously unsatisfactory in a programme of frequent tests. The requirements of sinusoidal testing, such as the need to both abstract as well as inject, formed the basis of the specifications for the system. It had also been discovered in previous testing that the location of the source zone signal required precise definition and should not be allowed to "spread" to the rest of the source borehole. This defined another of the characteristics of the system, the control of the head in the rest of the source zone borehole.

Based on previous experience, certain other system characteristics were incorporated into the equipment. These included such aspects as the ability to measure pressure within the source zone, the ability to check for and measure pressure transducer drift and the ability to seal the boreholes containing packer strings at their mouths.

The computer-controlled hydraulic testing system which was designed by B.G.S. and S.G.A.B. and built by S.G.A.B. is described in detail by Holmes

and Sehlstedt, (1987). It is unusual compared to all previous hydraulic testing equipment because the tests are actually controlled by the computer based on criteria supplied by the test operator. All previous equipment only used computers for data aquisition.

1.3 NEW INTERPRETATION

Sinusoidal pressure testing is a comparatively new concept in terms of the equipment used and the form of the measurements. It also has the disadvantage compared to more standard testing that there is no well-developed literature. An interpretation procedure has therefore had to be developed from first principles. An outline of the approach together with some simple flow geometrics was put forward by Black and others (1986). The importance of a sensible and appropriate flow geometry cannot be overstressed in a project designed to ascribe hydraulic properties to geometrical features defined by geophysics. This report describes the enlargement of the previous report (Black and others, 1986) to include a wider range of possible flow geometrics.

1.4 AIMS OF THIS REPORT

The aims of this report are broadly to summarize the use of sinusoidal pressure tests to evaluate the hydrogeology of the Crosshole Site at the Stripa Mine. The report is divided into sections describing the following aspects:

1) the design of the programme of sinusoidal tests
2) the performance of the tests [there is more detail in Holmes and Sehlstedt, 1987]
3) the results
4) the deviation of the theory of sinusoidal testing
5) the analysis of the tests
6) the interpretation of the meaning of the results in the context of the Crosshole Site

2 IMPLEMENTATION OF SINUSOIDAL TESTS

2.1 TEST STRATEGY

The crosshole sinusoidal tests were the last task carried out within the Crosshole Project. Consequently much information was already available concerning the distribution of the geophysical properties between the boreholes and the distribution of hydraulic properties along them. The choice in the testing strategy was between a form of "blanket" testing which would be very coarse, owing to constraints of time and cost, and a more focussed approach.

It would have been comparatively easy to pump each one of the boreholes in turn and measure the response of the other complete boreholes. However this would not have yielded any information about the particular between-borehole flow paths or where they intersected the boreholes. The opposite strategy of testing many short zones in a form of tomographic testing would have been clearly impossible. Indeed it would have been unwise to adopt an approach based on the wave equation for a technique based on the diffusion equation.

The procedure adopted was to test in the region of broad zones identified by the geophysical techniques (see Olsson and others, 1987). Whilst testing in the vicinity of these zones, the rest of the borehole and its neighbours were monitored for evidence of the source zone signal. Hence it was hoped to identify all significant crosshole connections in addition to those selected on the grounds of geophysics.

Although alternative "cocktails of frequencies" were discussed, it was decided to use single frequency sinusoids in all the testing. This was because of the strategy of using the longest period sinusoids first to identify the active regions with the most sensitive frequency. Hence once a responding pair of zones (source to receiver) was identified, it was comparatively quick to then test it at the higher frequencies. The idea of testing zones at various frequencies was retained in order to discover more about the hydraulic properties of conductive features.

The testing strategy can be summarised:

- select a geophysically identified zone in two boreholes and

place source and receiver strings appropriately

- carry out long period sinusoidal test (24hr period) and observe for responses in the receiver string including the long zones at the beginning and end of the receiver borehole
- observe for responses in other boreholes (if present then borehole can be connected to the "guard zone" of the source borehole or opened)
- if there are responses in the receiver zones then carry out higher frequency tests measuring only those previously responding zones. Increase frequency until there is no response.
- if there is no response
  either i) move source string to adjacent position within geophysical feasture
  ii) if all candidates already tested then move receiver string to new position in same geophysical feature
  iii) if all combinations checked then move source and receiver string to next feature in same pair of boreholes
  iv) if all combinations exhausted then move source string to new borehole
  v) repeat for same receiver borehole and then move receiver string

In general the testing was organised so that the source zone was moved rather than the receiver zone because this entailed less physical work (the receiver string contained 6 packers compared to the 2 of the source string). A systematic reversal of testing direction was not undertaken. It was the original intention to check results against a comparable series of "standard" tests but this was not possible in the time available. The complexity of the testing regime is probably apparent from the description above.

2.2 TEST IMPLEMENTATION

This section of the report provides an overview of the equipment and operational procedures used to perform sinusoidal tests. More detailed information can be found in Holmes and Sehlstedt, 1987.

2.2.1 Equipment description

All the equipment is self-contained and housed in the mine working area of the SGAB Drift some 360 metres below ground level. The various pumps, valves

and inflation equipment are positioned in the mine cavity only some metres from the array boreholes. A large cabin, constructed in one corner of the mine cavity, provides protection for the main control cabinet and microcomputer.

The source borehole contains two hydraulically inflated packers, which can be separated to produce a test zone from 1 to 20 metres in length. A rod string is used to position these in the borehole and also connects the source zone, between the packers, to pumps which inject or abstract water to create any required variation in pressure (called the hydraulic signal). The source zone pressure is monitored by a 35 Bar transducer located down-hole, immediately adjacent to the test section. A by-pass tube through the packer assembly connects the two lengths of borehole either side of the packers, jointly termed the rest-of-borehole zone. A transducer (35 Bar) measures the pressure of this zone.

All the rods, tubes and cables pass through a tapered sealing manifold. This device is bolted onto a flanged pipe which is grouted into the end of each of the boreholes within the array. Rubber elements are compressed by a pressure plate and seal around the pipes and tubes passing through the manifold. They can operate to a maximum pressure of 40 Bars and stop the source borehole from loosing pressure by water draining into the drift. The manifold is removed to re-locate the packer assembly, but can be refitted within 10 minutes. All other boreholes are sealed by plates during testing and their pressures monitored by 35 Bar transducers.

Two pumps operate in the mine working area. One injects or abstracts water from the source zone, under computer command, to generate hydraulic signals. The other responds to pressure changes in the rest of borehole zone caused by water flowing around the isolating packers. Any pressure fluctuations are damped out to ensure that the hydraulic signal originates from the source zone and is not derived from the leakage of the signal to the rest of borehole zone. Both pumps are, however, identically constructed. Each comprises a finely machined cylinder with a tightly fitting double-acting ram. This water pump is moved by a direct-coupled, hydraulic-augmented mechanical driving ram, the exact linear position of which is controlled by a stepping motor. Solenoid valves are fittted to the entrance and exit ports of the water cylinder to control the direction of flow, either into the borehole or to a storage reservoir. One step of the motor is 0.033 cm^3 of water. The flow rate ranges between 0.033 and 3000 cm^3/minute at up to 40 Bars, at which a pressure relief valve operates to protect the system against overpressurisation.

Each pump has an "on board" microprocessor, acting as an interface, which accepts commands from the central microcomputer to increase or decrease the flow rate. These are interpreted to vary the stepping rate and solenoid status to provide the required rate and direction of flow. The motor stepping rate is recorded by the control computer as a direct measure of flow rate, assuming there is no leakage around the water ram. Filters are provided to protect the pumps against particulate material which could damage the ram seals.

The receiver borehole contains six hydraulically inflated packers which isolate five short and two long zones. Each of these is connected to the mine area by a water filled pressure tube. The packer assembly is positioned by a "blank rod string" using a hydraulically powered handling device. All the tubes emerge from the borehole through a tapered sealing manifold, similar to the one on the source borehole, and continue to a "pressure measuring board".

The board comprises a group of solenoid-actuated valves and pressure transducers. The tube from each zone is isolated from the "pressure measuring board" by a solenoid-actuated "access valve". The pressure in the tube is measured by opening the appropriate "access valve" and hence connecting the tube directly to an absolute pressure transducer with a range up to 35 Bar. For more detailed measurement two differential transducers (1 and 7 Bar), which measure zone pressure relative to a variable reference pressure, are located in the system. The reference pressure is contained in a "reference pressure tube" which is actually a long plastic tube installed in a nearby mine shaft. The column of water in this tube, which has a free upper surface, can be varied in height to match the pressure in the receiver zones. This pressure is measured by another 35 Bar transducer.

The differential transducers allow zone pressures to be measured to a greater accuracy than is possible using absolute transducers. The 35 Bar (~350 m. water equivalent pressure) instrument can resolve to 0.1 metres with an accuracy (non-linearity and hysteresis) of +/-0.2m.. However, these values are 0.01 m. and 0.04 m. for the 7 Bar and 0.001 m. and 0.006 m. for the 1 Bar differential transducers. The reference pressure allows this accuracy to be maintained over a 0 to 35 Bar absolute pressure range. The differential transducers are easily damaged by excess pressure and need to be protected from connection to extremely different pressures.

Reading the pressure of each receiver zone follows an identical pattern, controlled by the main computer. Firstly the solenoid-actuated valves for a particular zone is opened to connect that zone to the absolute transducer. This pressure value is then compared to a pressure reading obtained from the reference tube. If they lie within 7 Bars, the 7 Bar differential transducer is switched into the measuring loop. Normally both differential transducers are isolated from the measuring loop and the pressure is balanced across the measuring head. If the pressure difference is less than 1 Bar, the 1 Bar differential instrument can be read. This process is repeated for each preselected zone pressure until a scan of all the zones has been completed.

Packers in both the source and receiver boreholes are inflated by a water system with a gas overpresure to a pressure of about 20 Bar in excess of the environmental pressure. Each inflation system is monitored by a 70 Bar transducer which is read by the central computer. Alarm values can be set by the operator (maximum or minimum) which, if passed, cause the computer to issue warnings. If no action is taken the testing system is automatically closed down. All the solenoid-actuated valves are closed to isolate the boreholes from water inflow or outflow. Thus, water will not drain into the mine causing borehole pressures to fall. Similar action results if there is a power failure in the mine.

The control system comprises a central Z80-based microcomputer driving a group of intelligent peripherals. The pumps and transducers are operated via processor-based units responding to simple command strings. This frees the central computer from time consuming control functions. Data are stored on floppy disc and can also be presented in "real time" on a matrix printer in graphical form.

The key element in testing is the ability of the control system to generate the hydraulic signal in the source zone. The central computer calculates a predicted sinusoidal curve based on information (amplitude, frequency etc.) provided by the operator. In the control cycle the computer compares the measured source zone pressure to the predicted and commands the pumps to increase or decrease the injection or abstraction rate to follow the curve. During testing this cycle is repeated, on average, every ten seconds. The rest-of-borehole pressure is controlled in a similar manner.

2.2.2 Performing sinusoidal tests

Sinusoidal testing is used as a means of determining hydraulic properties between boreholes, creating the signal in the source zone and monitoring the response, to receiver sections, in another borehole. A full testing sequence comprises several tests at different frequencies. Usually 24 hour, 12 hour, 4 hour and 40 minute periods were used, with occasionally a 10 minute period in very transmissive zones. The system can produce either sinusoidal flow rate or sinusoidal pressure. In most tests only the pressure was controlled as this produced a better form of curve.

Each separate sinusoidal test comprises three phases, the length of each being set by the operator. Firstly there is a monitoring phase, usually no more than 4 hours during which ambient pressure changes can be recorded. Secondly there is the active phase in which the source zone and rest of borehole pressures are manipuleted by the pumps. Three or more sinusoidal periods may be included in this phase. Lastly there is another passive phase for monitoring ambient pressure changes. The passive phases are important to record pressure changes generated by sealing and unsealing boreholes in the array.

The operator uses the following procedure to perform a sinusoidal test:

a) Locations for the source and receiver borehole packers are selected form the single borehole testing, radar, seismic and geophysics results.

b) Packers are installed at these locations and inflated to a suitable pressure.

c) The operator enters information on the desired sinusoid signal (amplitude, frequency, number of waves, duration of passive phases, measuring points etc) into the control computer. The first test in a new zone usually has a period of 1440 or 720 minutes. The test is started and occasionally monitored by the operator to ensure its correct implementation.

d) On completion of the test the results are analysed. If a positive signal has been received, the zone may be re-tested using a shorter wave period.

e) When sufficient information has been collected from the zone the packers are deflated and moved to new locations.

2.2.3 Checks on equipment effects

Various aspects of the equipment design have an influence on the interpretation of the results. Two important aspects are spread of the hydraulic signal and receiver zone response times. A third aspect, which became important during fractional dimension analysis, is the storage in the source borehole.

Spread of the hydraulic signal, generated in the source zone, via artificial pathways (boreholes) can produce responses where they would not occur in the natural system. For example, a signal generated in a fracture zone in one borehole could cause a fluctuation in an adjacent borehole. The entire length of this borehole would oscillate with the signal and retransmit it to another fracture zone. Spread of signal to the rest of the source borehole was stopped by the use of a second pump stabilising the pressure. Other boreholes were connected to this pump to damp out any transmitted signal.

Receiver zone response time is a measure of the packered interval to intercept a hydraulic signal in the surrounding rock. A long response time implies that a change occuring in the rock will not be measured in the zone until some time has passed. The ideal is a very short rsponse time in which pressures in the packered interval mirror those in the rock. It depends upon the transmissivity of the rock and the storage in the packered interval and measuring lines of the receiver system. A low storage implies that a small volume of water entering the packered interval will create a large pressure change. A high storage will produce a smaller pressure rise for the same volume of water. The volume of water which enters the zone for a given head difference depends on the rock transmissivity. The equipment was designed to have minimum storage, in the order of a few cubic centimetres, and was operated in highly transmisive zones. Thus the response times were small, usually less than 5 seconds, and could be ignored. Response times can be measured by performing a pulse test on the test section and using an analysis suggested by Black and Kipp (1977).

Source zone storage is a significant parameter in the calculation of flow characteristics using fractional dimensions. As this analysis was introduced after the completion of field testing no direct measurements were made at the time and values have had to be estimated. The storage is a measure of the change in volume required to cause a unit pressure change in the equipment comprising the source system. This includes the volume of water contained in the packered interval, in the rods and flexible lines and also in the source board and pumps.

The storage of the packered interval and rods was measured during the testing and can be accurately estimated for various configurations. However, the storage of the source boards and pumps is known to be variable due to the presence of gas pockets in the complicated pipework, caused by out-gassing of the water during the fluctuating pressure regime of sinusoidal tests. This variable storage necessitated the disconnection of the source board during pulse testing using the source borehole equipment. The likely range of system storage, given assumptions on gas volumes contained in the pipework and known working pressures, has been calculated at from 1 to 5 mm. (here expressing the storage as an equivalent open pipe radius). The most likely values are from 1.5 to 2.5 mm..

2.3 RESULTS

2.3.1 Preprocessing of the results

The computer recorded the source and receiver measurements and when there were responses they were of the form shown in Figure 2.1a. This is typical data in that the received signal is imposed on a gradually changing background environmental head. In order to derive the basic parameters, amplitude attenuation and phase lag, for analysis the raw data requires correcting for drift. This was achieved using a microcomputer program called "SINEFIT" and was carried out at the mine. In essence the program applies a drift correction and then performs a least squares fit of each signal to a sinusoid of period equal to the test. It then writes out amplitudes and phase lags of the receiver data relative to the source data and plots the resultant match (see Figure 2.1b). The program is detailed in Black and others, (1986).

2.3.2 Basic results

The results of the sinusoidal testing are given in Table 2.1. The table includes tests which were carried out within the respective zones but which did not yield measureable results. In particular boreholes F1 and E1 were searched for responses but none was found. The borehole F6 is ommitted from the results because there was no sinusoidal testing involving F6 owing to the low heads pertaining in that borehole. This was because the sinusoidal method was centred on equal volumes of injection and abstraction. Abstraction was not possible.

a) RAW DATA

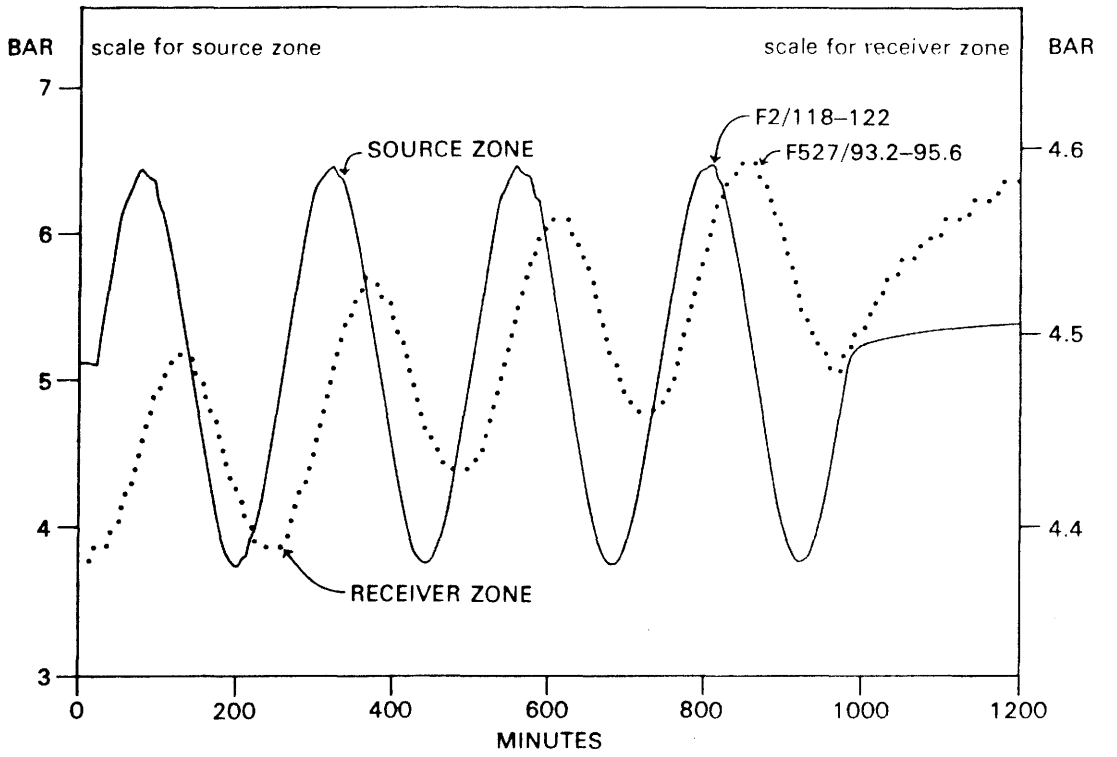

b) FITTED SINE WAVES BY "SINEFIT"

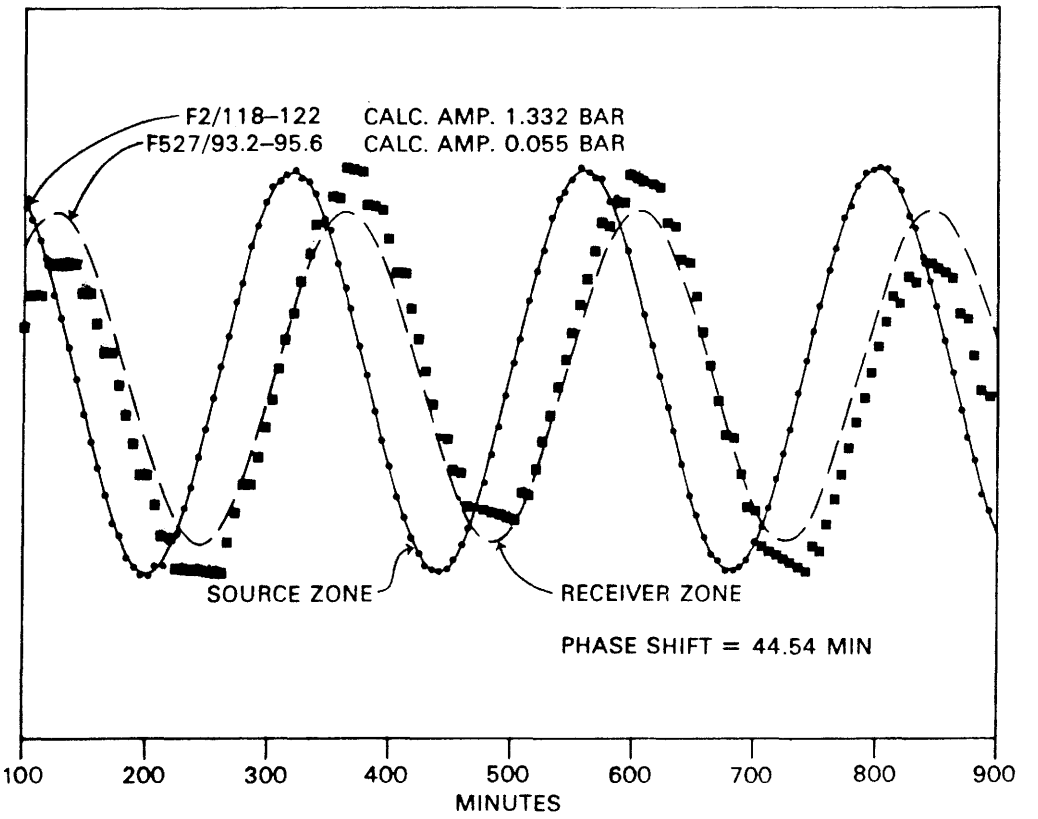

Figure 2.1 Manipulation of data to yield basic data of amplitude attenuation and phase shift
a) raw data b)fitted sine waves by "SINEFIT"

TABLE 2.1 Basic results from the sinusoidal testing

SOURCE BOREHOLE			RECEIVER BOREHOLE			period	Q	Ampl.	Angle
	position of zone (m)			position of zone (m)		(mins)	(l/min)	(m)	(°)
F2	0	250	F3	0	200	15		SOME RESPONSE	
			F5	0	200	15		SOME RESPONSE	
F5	0	200	F4	0	250	60		.027	83.8
			F2	0	250	60		.027	69.07
F2	0	250	F4	0	250	60		.210	42.8
			F5	0	200	60		.01	72.9
			F3	0	200	60		.033	58.6
			F1	0	200	60		NO RESPONSE	
			E1	0	300	60		.006	73.1
F1	0	200	F4	0	250	60		NO RESPONSE	
			F5	0	200	60		NO RESPONSE	
			F2	0	250	60		NO RESPONSE	
			F3	0	200	60		NO RESPONSE	
			E1	0	300	60		NO RESPONSE	
F2	0	250	F4	0	250	15		.18	55.9
			F5	0	200	15		NO RESPONSE	
			F3	0	200	15		.022	89.5
			F1	0	200	15		NO RESPONSE	
			E1	0	300	15		NO RESPONSE	
F3	40.0	44.0	F5	45.05	200	720	.09	.011	78.6
			F5	41.50	43.90			.059	90.1
			F5	37.95	40.35			.183	40.2
			F5	34.4	36.8			.023	93.4
			F5	30.85	33.25			NO RESPONSE	
			F5	27.3	29.7			NO RESPONSE	
F3	40.0	44.0	F5	37.95	40.35	12	.10	.023	40.56
F3	40.0	44.0	F5	62.8	200	240	.09	NO RESPONSE	
			F5	59.25	61.65			NO RESPONSE	
			F5	55.7	58.1			NO RESPONSE	
			F5	52.15	54.55			NO RESPONSE	
			F5	48.6	51.0			NO RESPONSE	
			F5	45.05	47.45			NO RESPONSE	
			F5	0	43.9			SOME RESPONSE	
F3	103.0	107.0	F5	96.75	200	1440	.25	.026	73.49
			F5	93.2	95.6			.305	17.54
			F5	89.65	92.05			.214	56.07
			F5	86.1	88.5			.188	65.81
			F5	82.55	84.95			.162	75.03
			F5	79.0	81.4			.056	117.58
			F5	0	77.85			.009	59.4
			F1	0	200			.025	33.66
			F2	0	250			.157	12.72
F3	103.0	107.0	F5	96.75	200	240	.38	.004	98.9
			F5	93.2	95.6			.228	26.6

TABLE 2.1 (Continued)

SOURCE BOREHOLE			RECEIVER BOREHOLE			period	Q	Ampl.	Angle
	position of zone (m)			position of zone (m)		(mins)	(l/min)	(m)	(°)
			F5	89.65	92.05			NO RESPONSE	
			F5	86.1	88.5			NO RESPONSE	
			F5	82.55	84.95			NO RESPONSE	
			F5	79.0	81.4			NO RESPONSE	
			F5	0	77.85			SOME RESPONSE	
			F1	0	200			.009	70.7
			F2	0	250			.104	26.3
F3	103.0	107.0	F5	96.75	200	60	.55	NO RESPONSE	
			F5	93.2	95.6			.098	55.9
F3	103.0	107.0	F5	96.75	200	40	1.1	NO RESPONSE	
			F5	93.2	95.6			.098	55.9
			F4	0	77.85			NO RESPONSE	
F3	103.0	107.0	F5	93.2	95.6	8		NO RESPONSE	
F3	112.0	116.0	F5	96.75	200	720	.07	NO RESPONSE	
			F5	93.2	95.6			.025	35.09
			F5	89.65	92.05			NO RESPONSE	
			F2	0	250			NO RESPONSE	
F2	44.0	48.0	F5	96.75	200	1440	.045	NO RESPONSE	
			F5	93.2	95.6			.009	81.08
			F5	0	77.85			.035	47.99
			F4	0	250			.24	8.34
			F3	0	200			.015	59.99
F2	118.0	122.0	F5	96.75	200	240	.18	NO RESPONSE	
			F5	93.2	95.6			.058	69.01
			F5	0	77.85			.016	86.15
			F4	0	250			NO RESPONSE	
			F3	0	200			.137	39.41
F2	118.0	122.0	F5	96.75	200	40	.15	NO RESPONSE	
			F5	93.2	95.6			.0054	134.3
			F5	0	77.85			NO RESPONSE	
			F4	0	250			NO RESPONSE	
			F3	0	200			.039	54.96
F4	124.0	128.0	F5	96.75	200	1440	.09	NO RESPONSE	
			F5	93.2	95.6			.005	140.7
			F5	0	77.85			NO RESPONSE	
			F2	0	250			NO RESPONSE	
			F3	0	200			NO RESPONSE	
F4	124.0	128.0	F5	96.75	200	240	.09	NO RESPONSE	
			F5	93.2	95.6			NO RESPONSE	
			F5	0	77.85			NO RESPONSE	
			F2	0	250			NO RESPONSE	
			F3	0	200			NO RESPONSE	
F4	52.0	56.0	F5	96.75	200	1440	.13	.007	125.6

TABLE 2.1 (Continued)

SOURCE BOREHOLE position of zone (m)			RECEIVER BOREHOLE position of zone (m)			period (mins)	Q (l/min)	Ampl. (m)	Angle (°)
			F5	93.2	95.6			.083	68.02
			F5	89.65	92.05			.0152	96.24
			F5	86.1	88.5			.016	21.71
			F5	82.55	84.95			.022	22.46
			F5	79.0	81.4			NO RESPONSE	
			F5	0	77.85			.12	42.04
			F2	0	250			.469	5.33
			F3	0	200			.117	39.53
F4	52.0	56.0	F5	96.75	200	240	.17	NO RESPONSE	
			F5	93.2	95.6			.021	92.82
			F5	89.65	92.05			NO RESPONSE	
			F5	86.1	88.5			NO RESPONSE	
			F5	82.55	84.95			.008	55.28
			F5	79.0	81.4			NO RESPONSE	
			F5	0	77.85			.068	49.63
			F2	0	250			.372	9.47
			F3	0	200			.055	57.42
F4	52.0	56.0	F5	93.2	95.6	40	.35	NO RESPONSE	
			F5	0	77.85			.029	63.92
			F2	0	250			.368	17.16
			F3	0	200			.019	88.14
F4	52.0	56.0	F5	51.75	200	1440	.20	NO RESPONSE	
			F5	48.2	50.6			.063	45.84
			F5	44.65	47.05			NO RESPONSE	
			F5	41.1	43.5			.077	34.38
			F5	37.55	39.95			.066	44.90
			F5	34.0	36.4			NO RESPONSE	
			F5	0	32.85			NO RESPONSE	
F4	52.0	56.0	F5	51.75	200	240	.10	NO RESPONSE	
			F5	48.2	50.6			.038	74.85
			F5	44.65	47.05			NO RESPONSE	
			F5	41.1	43.5			NO RESPONSE	
			F5	37.55	39.95			.044	54.97
			F5	34.0	36.4			NO RESPONSE	
			F5	0	32.85			NO RESPONSE	
			F2	0	250			.372	8.49
			F5	0	200			.044	52.97
F4	52.0	56.0	F5	48.2	50.6	40	.19	.007	104.55
			F5	37.55	39.95			.014	58.57
			F2	0	250			.252	16.20
			F5	0	200			.009	85.75
F4	52.0	56.0	F5	37.55	39.95	12		NO RESPONSE	
F2	44.0	48.0	F5	51.75	200	1440	.19	.076	47.79
			F5	48.2	50.6			.116	66.76
			F5	44.65	47.05			.053	114.43
			F5	41.1	43.5			.063	102.31

TABLE 2.1 (Continued)

SOURCE BOREHOLE position of zone (m)			RECEIVER BOREHOLE position of zone (m)			period (mins)	Q (l/min)	Ampl. (m)	Angle (°)
			F5	37.55	39.95			.12	61.74
			F5	34.0	36.4			.035	116.9
			F5	0	32.85			.081	57.66
			F2	0	250			.251	13.15
			F5	0	200			.237	15.48
F2	44.0	48.0	F5	51.75	200	240	.20	.037	64.06
			F5	48.2	50.6			.033	78.64
			F5	44.65	47.05			.006	137.3
			F5	41.1	43.5			NO RESPONSE	
			F5	37.55	39.95			.036	60.54
			F5	34.0	36.4			.007	129.37
			F5	0	32.85			.027	72.92
			F3/F4	0	250			.220	19.64
F2	44.0	48.0	F5	48.2	50.6	40	.19	.005	102.8
			F5	44.65	47.05			NO RESPONSE	
			F5	41.1	43.5			NO RESPONSE	
			F5	37.55	39.95			.007	47.25
			F5	34.0	36.4			NO RESPONSE	
			F5	0	32.85			NO RESPONSE	
			F3/F4	0	250			.085	7.79
F1	93.45	97.45	E1	78.45	200	240	.058	NO RESPONSE	
			E1	71.35	73.75			NO RESPONSE	
			E1	67.8	70.0			NO RESPONSE	
			E1	64.25	66.65			NO RESPONSE	
			E1	60.75	63.15			NO RESPONSE	
			F2	0	250			NO RESPONSE	
			F3	0	200			NO RESPONSE	
F1	93.45	97.45	E1	149.9	152.3	40	.03	NO RESPONSE	
			E1	146.35	148.75			NO RESPONSE	
			E1	142.8	145.2			NO RESPONSE	
F1	93.45	97.45	E1	153.45	200	240	.05	NO RESPONSE	
			E1	149.9	152.3			NO RESPONSE	
			E1	146.35	148.75			NO RESPONSE	
			E1	142.8	145.2			NO RESPONSE	
			E1	139.25	141.65			NO RESPONSE	
			E1	135.7	138.1			NO RESPONSE	
			E1	0	134.0			NO RESPONSE	
F4	191.0	250	F2	211.15	250	2160	.09	NO RESPONSE	
			F2	207.6	210.0			NO RESPONSE	
			F2	204.05	206.45			NO RESPONSE	
			F2	200.5	202.9			NO RESPONSE	
			F2	196.95	199.35			NO RESPONSE	
			F2	193.4	195.8			NO RESPONSE	
			F2	0	192.0			NO RESPONSE	
			F3/F5	0	250			NO RESPONSE	
F3	151.0	200	F2	211.15	250	1440	.05	NO RESPONSE	

TABLE 2.1 (Continued)

SOURCE BOREHOLE position of zone (m)			RECEIVER BOREHOLE position of zone (m)			period (mins)	Q (l/min)	Ampl. (m)	Angle (°)
			F2	207.6	210.0			NO RESPONSE	
			F2	204.05	206.45			NO RESPONSE	
			F2	200.5	202.9			NO RESPONSE	
			F2	196.95	199.35			NO RESPONSE	
			F2	193.4	195.8			NO RESPONSE	
			F2	0	192.0			NO RESPONSE	
			F4	0	250			NO RESPONSE	
F3	151.0	200	F5	145.2	200	1440	.05	NO RESPONSE	
			F5	141.65	144.05			.018	353.75
			F5	138.1	140.5			NO RESPONSE	
			F5	134.55	136.95			NO RESPONSE	
			F5	131.0	133.4			NO RESPONSE	
			F5	127.45	129.85			NO RESPONSE	
			F5	0	126.3			NO RESPONSE	
			F2/F4	0	250			NO RESPONSE	
F3	106.0	110.0	F2	127	250	1440	.25	NO RESPONSE	
			F2	123	126			.226	8.24
			F2	116	119			.500	18.0
			F2	113	115			.283	36.0
			F2	109	112			.275	36.0
			F5	0	200			SLIGHT RESPONSE	
			F1	0	200			NO RESPONSE	
F3	130	200	F5	145.2	200	1440	.05	NO RESPONSE	
			F5	141.65	144.05			SLIGHT RESPONSE	
			F5	138.1	140.5			NO RESPONSE	
			F5	134.55	136.95			NO RESPONSE	
			F5	131.0	133.4			NO RESPONSE	
			F5	127.45	129.85			NO RESPONSE	
			F5	0	126.3			NO RESPONSE	
			F2/F4	0	250			NO RESPONSE	
F3	130	200	F2	211.15	250	1440	.05	.006	203.97
			F2	207.6	210.0			NO RESPONSE	
			F2	204.05	206.45			.006	205.85
			F2	200.5	202.9			.004	188.56
			F2	196.95	199.35			NO RESPONSE	
			F2	193.4	195.8			NO RESPONSE	
			F4	0	250			NO RESPONSE	
F3	100	200	F5	145.2	200	600	.25	NO RESPONSE	
			F5	141.65	144.05			.034	90.98
			F5	138.1	140.5			NO RESPONSE	
			F5	134.55	136.95			NO RESPONSE	
			F5	131.0	133.4			NO RESPONSE	
			F5	127.45	129.85			NO RESPONSE	
			F5	0	126.3			.025	77.68
			F2/F4	0	250			.073	41.38
F3	99.2	200	F4	205.7	250	1440	.30	NO RESPONSE	
			F4	202.15	204.55			.013	324.36
			F4	198.6	201.0			.003	356.06

TABLE 2.1 (Continued)

SOURCE BOREHOLE position of zone (m)			RECEIVER BOREHOLE position of zone (m)			period (mins)	Q (l/min)	Ampl. (m)	Angle (°)
			F4	195.5	197.45			.003	8.74
			F4	191.5	193.9			.009	13.35
			F4	0	190.35			.16	28.82
			F5	0	200			.054	57.93
F3	37.3	41.3	F4	60.45	250	720	.11	.023	5.73
			F4	56.9	59.3			NO RESPONSE	
			F4	53.35	55.75			.016	10.08
			F4	49.8	52.2			.006	16.87
			F4	46.25	48.65			NO RESPONSE	
			F4	0	250			SLIGHT RESPONSE	
F3	37.3	41.3	F4	60.45	250	240	.11	.014	18.19
			F4	53.35	55.75			.009	4.56
			F4	49.8	52.2			SLIGHT RESPONSE	
			F4	46.25	48.65			NO RESPONSE	
			F5	0	250			SLIGHT RESPONSE	
F3	37.3	41.3	F4	60.45	250	60	.08	.003	33.82
			F4	56.9	59.3			NO RESPONSE	
			F4	53.35	55.75			.007	12.08
			F4	49.8	52.2			NO RESPONSE	
			F4	46.25	48.65			NO RESPONSE	
			F4	0	250			NO RESPONSE	
F3	37.3	41.3	F4	60.45	250	40	.11	.015	41.65
			F4	53.35	55.75			.016	7.96
			F4	49.8	52.2			NO RESPONSE	
F3	37.3	41.3	F4	60.45	250	10	.11	.004	113.96
			F4	53.35	55.75			.009	28.41
			F4	49.8	52.2			NO RESPONSE	
F3	37.3	41.3	F4	75.45	250	1320	.11	NO RESPONSE	
			F4	71.9	74.3			NO RESPONSE	
			F4	68.35	70.75			NO RESPONSE	
			F4	64.8	67.2			NO RESPONSE	
			F4	61.25	63.65			NO RESPONSE	
			F4	0	60.1			.0058	343.87
F3	103.3	107.3	F4	114.45	250	720	.31	NO RESPONSE	
			F4	110.9	113.3			NO RESPONSE	
			F4	107.35	109.75			NO RESPONSE	
			F4	103.8	106.2			NO RESPONSE	
			F4	100.25	102.65			NO RESPONSE	
			F4	0	99.1			.011	4.76
F5	37.3	41.3	F4	60.45	250	720	.75	.332	13.26
			F4	56.9	59.3			NO RESPONSE	
			F4	53.35	55.75			.172	3.78
			F4	49.8	52.2			.128	30.95
			F4	46.25	48.65			.077	70.01
			F4	0	250			NO RESPONSE	

TABLE 2.1 (Continued)

SOURCE BOREHOLE	position of zone (m)		RECEIVER BOREHOLE	position of zone (m)		period (mins)	Q (l/min)	Ampl. (m)	Angle (°)
F2	43.3	47.3	F4	60.45	250	480	.11	.177	8.37
			F4	56.9	59.3			NO RESPONSE	
			F4	53.35	55.75			.581	2.00
			F4	49.8	52.2			.478	25.40
			F4	46.25	48.65			.367	61.59
			F4	0	250			NO RESPONSE	
F2	43.3	47.3	F4	60.45	250	40	.19	.141	27.70
			F4	53.35	55.75			.669	5.47
			F4	0	250			NO RESPONSE	
F2	43.3	47.3	F4	53.35	55.75	10	.43	.654	11.72
F2	118.3	122.3	F4	60.45	250	480	.11	NO RESPONSE	
			F4	56.9	59.3			NO RESPONSE	
			F4	53.35	55.75			NO RESPONSE	
			F4	49.8	52.2			NO RESPONSE	
			F4	46.25	48.65			NO RESPONSE	
			F4	0	250			NO RESPONSE	
F2	118.3	122.3	F4	114.45	250	720	.31	NO RESPONSE	
			F4	110.9	113.3			NO RESPONSE	
			F4	107.35	109.75			NO RESPONSE	
			F4	103.8	106.2			NO RESPONSE	
			F4	100.25	102.65			NO RESPONSE	
			F4	0	99.1			NO RESPONSE	
F5	37.3	41.3	F4	60.45	250	60	1.90	.230	40.37
			F4	53.35	55.75			.102	27.29
F5	37.3	41.3	F4	60.45	250	10	1.90	.027	33.58
F5	49.3	53.3	F4	60.45	250	30	.05	NO RESPONSE	
			F4	53.35	55.75			NO RESPONSE	
F5	94.3	98.3	F4	135.45	250	720	.07	NO RESPONSE	
			F4	131.9	134.3			NO RESPONSE	
			F4	128.35	130.75			NO RESPONSE	
			F4	124.8	127.2			NO RESPONSE	
			F4	121.25	123.65			NO RESPONSE	
			F4	0	120.1			NO RESPONSE	
F5	37.3	41.3	F3	48.45	200	720	.30	NO RESPONSE	
			F3	44.9	47.3			.306	4.92
			F3	41.35	43.75			.202	55.94
			F3	37.8	40.2			.365	5.56
			F3	34.25	36.65			.151	57.07
			F3	0	33.1			.008	47.25
F5	37.3	41.3	F3	48.45	200	240	1.30	NO RESPONSE	
			F3	44.9	47.3			.450	11.39
			F3	41.35	43.75			.195	64.99
			F3	37.8	40.2			.554	8.01

TABLE 2.1 (Continued)

SOURCE BOREHOLE position of zone (m)			RECEIVER BOREHOLE position of zone (m)			period (mins)	Q (l/min)	Ampl. (m)	Angle (°)
			F3	34.25	36.65			.195	64.13
			F3	0	33.1			.008	77.25
F5	37.3	41.3	F3	44.9	47.3	60	1.0	.185	37.24
			F3	41.35	43.75			.081	88.02
			F3	37.8	40.2			.238	15.56
			F3	34.25	36.65			.093	70.37
F5	37.3	41.3	F3	44.9	47.3	10	.70	.027	101.01
			F3	41.35	43.75			NO RESPONSE	
			F3	37.8	40.2			.059	52.04
F5	13.3	17.3	F3	48.45	200	360	.06	.099	23.35
			F3	44.9	47.3			.115	22.78
			F3	41.35	43.75			.118	23.06
			F3	37.8	40.2			.061	23.78
			F3	34.25	36.65			.062	30.23
			F3	0	33.1			.597	10.37
F2	43.3	47.3	F3	44.9	47.3	60	.24	.009	55.9
			F3	41.35	43.75			.009	56.07
			F3	34.25	36.65			.008	42.34
F2	43.3	47.3	F3	48.45	200	720	.20	NO RESPONSE	
			F3	44.9	47.3			.004	25.92
			F3	41.35	43.75			.004	24.29
			F3	37.8	40.2			.011	2.47
			F3	34.25	36.65			.009	17.27
			F3	0	33.1			.007	10.85
F2	118.3	122.3	F3	117.55	200	720	.12	.017	60.76
			F3	113.90	116.30			.169	39.31
			F3	110.35	112.75			.167	39.61
			F3	106.8	109.2			.173	37.31
			F3	103.35	105.75			.153	51.13
			F3	0	102.1			NO RESPONSE	
F2	118.3	122.3	F3	117.55	200	240	.12	.009	67.23
			F3	113.90	116.30			.111	49.12
			F3	110.35	112.75			.108	48.87
			F3	106.8	109.2			.116	44.50
			F3	103.35	105.75			.096	61.64
			F3	0	102.1			NO RESPONSE	
F2	118.3	122.3	F3	113.90	116.30	60	.16	.043	69.67
			F3	110.35	112.75			.042	70.85
			F3	106.8	109.2			.047	57.56
			F3	103.35	105.75			.039	77.75
F2	118.3	122.3	F3	106.8	109.2	15	.24	.017	79.37

This table shows 172 responses including mltiple responses between the same two zones at different frequencies. The tests were quite time consuming because it was necessary to chect the tests for responses **via** other boreholes. This was only possible because of the monitoring of the other boreholes and the ability of the test equipment to stop "signal spread" in the source borehole. However when this checking was carried out it reduced the number of "real" responses from 172 to 47. These are listed (see Table 2.2) according to the geophysically defined zone which was suspected to be present in the vicinity of the emplaced straddle intervals.

2.3.3 Qualitative interpretation

Zone A was the most extensively tested of all the geophysical zones by the crosshole sinusoidal technique. The places where responses were observed are shown in Figure 2.2. It can be seen that Zone A has more responses in the southern part of the Crosshole site (i.e. the right hand side of the diagram). This may indicate that Zone A is bifurcating in this direction. It should be noted that F2 and F1 are very close together at the northern end of the site and extensive searching of F1 yielded no responses. If Zone A penetrates to the north of the site it is not conductive in that region.

The other zone which was extensively tested was Zone C. Since it intercepts the boreholes further from the instrument drift the distances between the boreholes are larger than applies to Zone A. However, if anything, the number of responses seems to increase towards the north rather than the opposite in Zone A.

It is dangerous to overinterpret these basic results when the responses have not been checked against what would be expected assuming some simple flow geometries. There is a need for quantitative interpretation.

Table 3-4 Results from the sinusoidal testing

source-receiver boreholes	zone identifiers [separation] (m)	DETAILS OF SINE WAVE AT SOURCE period (minutes)	peak flow (m^3/sec) [x 10^6]	peak head (m)	flow/head phase shift (degrees)	RECEIVED SIGNAL peak head (m)	phase shift (degrees)
GEOPHYSICAL ZONE A							
4 -> 5	c - b [27]	1440	3.5	9.89	2.7	0.666	48
		240	2.5	9.94	17	0.442	73
	+++	240	3.0	10	2	0.327	40
		60	37	6.61	27	1.03	54
		10	35	3.9	31	0.269	65
	c - c [27]	1440	3.5	9.89	2.7	0.769	37
	c - d [26]	1440	3.5	9.89	2.7	0.625	49
		240	2.5	9.94	17	0.368	92
	+++	240	3.0	10	2	0.257	54
3 -> 4	b - c [23]	720	1.8	9.7	3	0.157	5
		240	1.9	9.64	3	0.087	66
		40	1.9	9.66	6	0.158	14
		10	1.9	9.72	11	0.095	39
2 -> 4	a -c [15]	480	2.0	9.74	9	5.8	15
		40	3.2	10.2	47	6.6	52
		10	7.1	12.72	52	6.5	64
	a - b [12]	480	2.0	9.74	9	4.7	34
	a - a [12]	480	2.0	9.74	9	3.67	71
3 -> 5	b - a [14]	720	1.7	9.66	11	0.23	104
	b - b [14]	720	1.7	9.66	11	1.83	51
		12	1.7	8.65	8	0.23	49
		6	1.4	9.43	20	0.099	60
	b - c [15]	720	1.7	9.66	11	0.59	101
2 -> 3	a - a [14]	720	3.3	8.95	3	0.09	20
		60	4.0	9.66	22	0.08	64
	a - b [13]	720	3.3	8.95	3	0.11	28
		60	4.0	9.66	22	0.10	56
	a - c [12]	720	3.3	8.95	3	0.036	27
		60	4.0	9.66	22	0.09	78
	a - d [12]	720	3.3	8.95	3	0.041	29
		60	4.0	9.66	22	0.09	78

Table 3.4 continued

source-receiver boreholes	zone identifiers [separation] (m)	DETAILS OF SINE WAVE AT SOURCE period (minutes)	peak flow (m^3/sec x 10^6)	peak head (m)	flow/head phase shift (degrees)	RECEIVED SIGNAL peak head (m)	phase shift (degrees)
GEOPHYSICAL ZONE C							
2 -> 5 -+-	e - e[64]	240	3.1	13.31	12.9	0.578	81.7
-+-		40	2.6	8.79	30.3	0.068	163.8
3 -> 5	e - e [36]	1440	3.9	7.28	18.6	3.05	36.1
		60	9.4	5.32	56.5	0.984	112.5
		40	18.1	5.69	59.1	0.82	138.2
		40	20.1	8.26	65.2	1.14	132.9
	g - e [41]	720	1.2	9.36	1.9	0.125	32.3
3 -> 2 ***	f - b [28]	1440	5.1	8.43	12.5	2.75	48.5
***	f - c [29]	1440	5.1	8.43	12.5	2.80	48.0
***	f - d [30]	1440	5.1	8.43	12.5	4.99	30.5
***	f - e [31]	1440	5.1	8.43	12.5	4.97	20.8
***	f - f [33]	1440	5.1	8.43	12.5	2.26	21.3
2 -> 3	e - f [31]	720	1.9	9.46	12.5	1.7	49.7
		240	2.0	9.45	16.5	1.2	61.0
		60	2.7	9.90	30.5	0.47	87.8
		15	4.5	10.76	35.5	0.17	14.6

Notes
+++ = not processed by SINEFIT due to errors in file header
-+- = probably transmitted through borehole F3
*** = test lasted less than one cycle

Positions of identified zones

zone labels	position of labelled zone in borehole (distances in m from collar) F2	F3	F4	F5
a	43.3 - 47.3	34.3 - 36.7	46.3 - 48.7	34.4 - 36.8
b	105 - 112	37.8 - 40.2	49.8 - 52.2	38.0 - 40.4
c	113 - 115	41.4 - 43.8	53.4 - 55.8	41.5 - 43.9
d	116 - 119	44.9 - 47.3		48.2 - 50.6
e	116 - 123	103 - 106		93.2 - 95.6
f	123 - 126	107 - 109		
g		110 - 116		

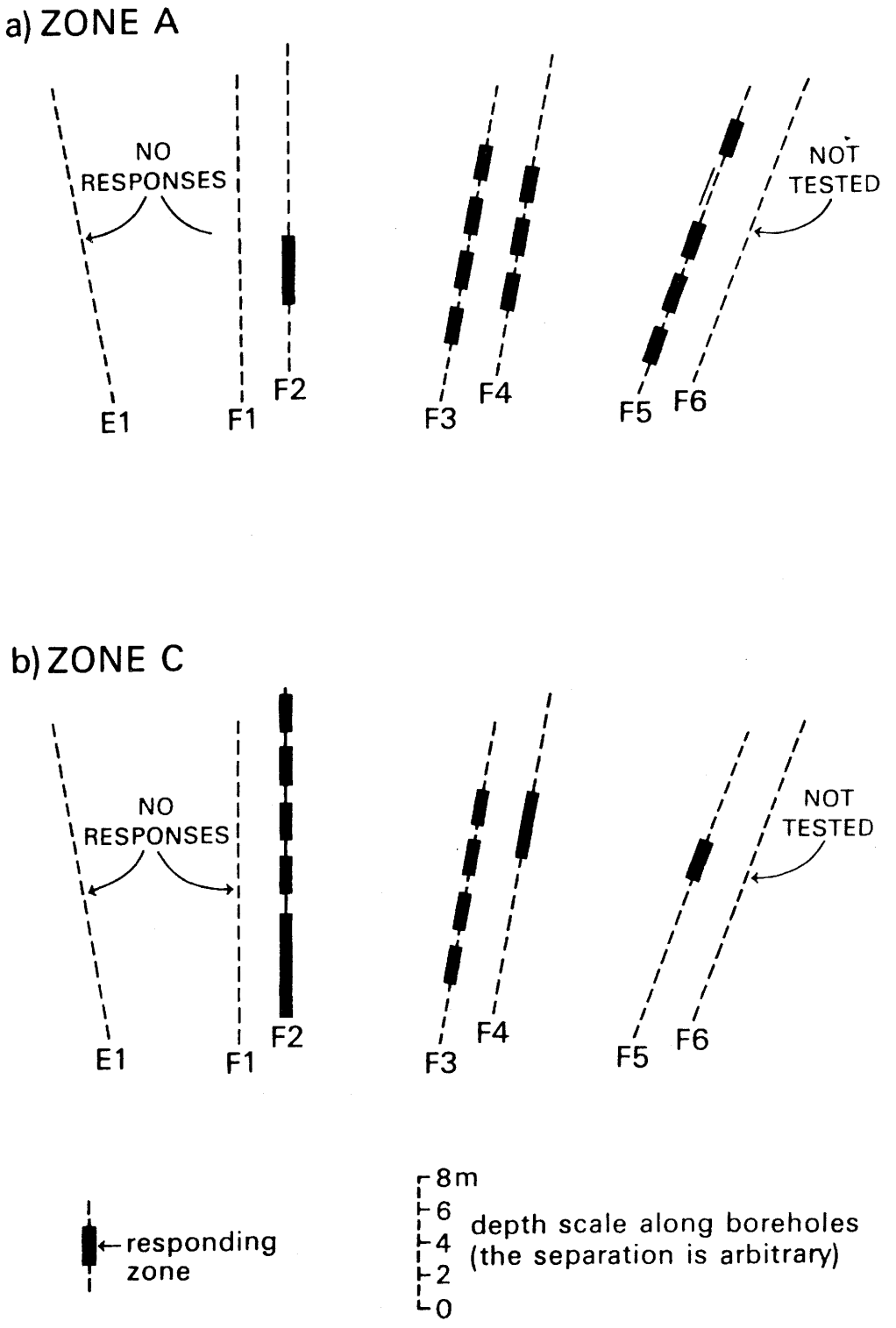

Figure 2.2 Pseudo-perspective plan of the intervals where crosshole responses were measured: a) Zone A b) Zone C

3. INTERPRETATION OF SINUSOIDAL TESTS

3.1 THEORY

3.1.1 Introduction

This section shows how the examination of the data derived from the tests has suggested the need for some new and complex concepts of flow in fractured rocks.

The models commonly used to describe hydraulic tests in groundwater systems with intergranular flow have an underlying assumption of radial flow from a borehole. Usually this is cylindrical flow as a result of either a large anisotropy or low permeability bounding strata. Sometimes, however, quasi-spherical flow is a more appropriate assumption, particularly for double-packer tests where the straddle interval is short.

In a previous report (Black and others, 1986) both the cylindrical and spherical models were developed for application to the data from sinusiodal pressure tests in the Stripa mine. Both forms were considered because it was unclear which form was more appropriate for use in a fissured rock environment. It was hoped that test results would indicate a preference for one of the models. However, in practice neither model has proved capable of satisfactorily reproducing the pressure variations observed in the Stripa Mine data. This difficulty has led to the development of a "generalized radial flow model" (Barker, in press) which can be applied to all standard forms of pumping test. For this report, this new model is presented in a form appropriate to the sinusoidal tests, and the results of applying it to test data from the Stripa mine are described.

On a scale that is much larger than the mean distance between fractures it is expected that flow can be described in terms of a homogeneous dual porosity medium. This is the conceptual basis for the spherical model found in Black and others,1986, and the main results are summarized here. As the scale of observation reduces with respect to the fracture spacing, it is to be expected that the structure of individual fracture zones will become important. A solution for flow in a single planar fissure was also discussed in Black and others,1986, and this will also be summarized and some important characteristics of the solution described. At even smaller scales it is widely believed (e.g. Abelin and others, 1985) that flow is confined to individual channels within a fracture zone, and the structure of these channels will then

become important. A solution for the flow in a single pipe-like channel embedded in matrix will be given in this report.

The development of models for the flow concepts described above requires the use of very restricted geometries for the fracture system. Thus, for example, only a planar fracture or a cylindrical tube channel can be treated, and in order to include minor offshooting fractures and channels the "matrix" properties must be chosen appropriately. The "matrix" component is also expected to encompass any irregularity in the fracture geometry. It is proposed here that an alternative way to generalize these models is to allow the dimensionality of the fracture system to assume any real value in the range 1-3 . To understand what is meant by this consider each of the previous models in turn. In the initial model of a homogeneously fractured dual porosity medium, the flow in the fracture system is assumed to be spherically symmetric, or three dimensional. In the single fissure case, flow is assumed to be radially symmetric within the fracture plane, so that the fracture system is two dimensional. Finally, in the channel case the fracture system is represented by a single pipe and the flow is one dimensional. All these cases can be written down using the same flow equation if the dimensionality is included as an integer variable taking the values 1,2 or 3. The generalization considered in this report is to allow the variable representing the dimensionality of the fracture system to take fractional, rather than integer, values between 1 and 3. The symbols used in this report are generally conventional, and are listed in full in Appendix C.

3.1.2 Homogeneous dual-porosity medium (3-D)

For completeness, the equations describing flow in an homogeneous dual-porosity medium are summarized from Black and others,1986. Combining Darcy's law with the conservation of mass equation for the fissures gives:

$$S_{sf}\frac{\partial h_f}{\partial t} = q + K_f\nabla^2 h_f = q + \frac{K_f}{r^2}\frac{\partial}{\partial r}\left[r^2\frac{\partial h_f}{\partial r}\right] \qquad 3.1$$

Black and others(1986) considered the solution of this equation with a sinusoidally varying point source and an interacting matrix component. The flow in the matrix was governed by the equation :

The flow in the matrix was governed by the equation :

$$S_{sm} \frac{\partial h_m}{\partial t} = K_m \frac{\partial^2 h_m}{\partial z^2} \qquad 3.2$$

The solution of these equations was obtained by the separation of variables. Thus, the solution was written in the form:

$$h_f(r,t) = R(r)\, e^{i\omega t} \qquad 3.3$$
$$h_m(r,z,t) = Z(r,z)\, e^{i\omega t}$$

The boundary conditions required to obtain the solution are, for the fractures

$$\lim_{r \to \infty} R = 0 \qquad 3.4$$

$$\lim_{r \to 0} 4\pi r^2 K_f \frac{\partial R}{\partial r} = -Q_0 \qquad 3.5$$

and for the matrix flow:-

$$q = -\frac{K_m}{(a+b)} \frac{\partial Z(r,a)}{\partial z} \qquad 3.6$$

and no flow at the centre of a matrix block.

It was shown that the solution can be written as :-

$$R = \frac{Q_0}{4\pi K_f r} e^{-\lambda r} \qquad 3.7$$

where λ contains terms with the properties of both fracture and matrix components of the rock mass. Figure 3.1 shows a sample curve of the variation of amplitude and phase with frequency predicted by equation 3.7 and Figure 3.2 shows the variations with distance.

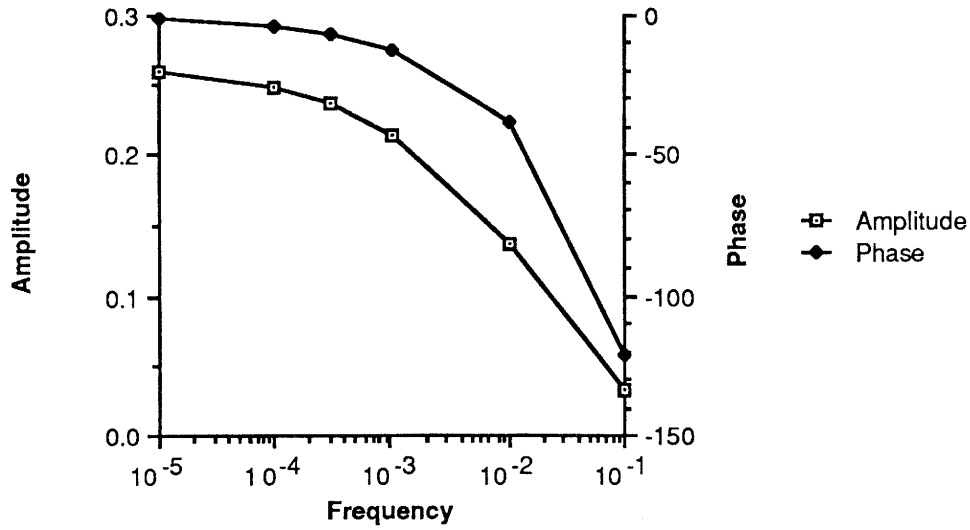

Figure 3.1 Variation of amplitude and phase shift with frequency for a three dimensional fissure flow system.

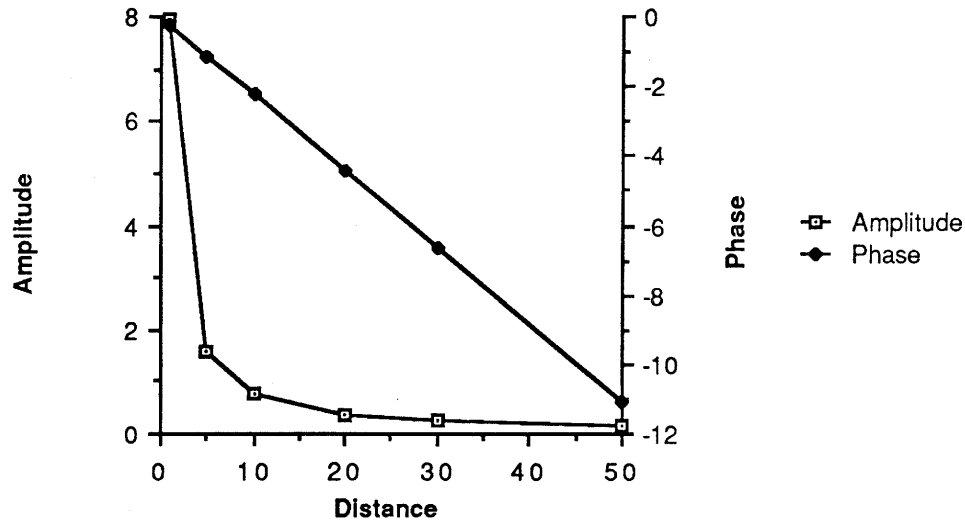

Figure 3.2 The variation of amplitude and phase shift with distance for a three dimensional flow system

3.1.3. Single fracture (2-D)

The equations of flow for a single fracture were also given in Black and others, 1986. For this case equation 3.1 becomes

$$S_{sf}\frac{\partial h_f}{\partial t} = q + \frac{K_f}{r}\frac{\partial}{\partial r}\left[r\frac{\partial h_f}{\partial r}\right] \qquad 3.8$$

The flow in the matrix is still given by equation 3.2 and the boundary condition 3.4 still holds, but instead of using the no flow boundary condition at the centre of a matrix block it is more appropriate to specify zero amplitude as $z\rightarrow\infty$.

The source boundary for the fissure system, equation 3.5, becomes

$$\lim_{r \to 0} 2\pi r K_f \frac{\partial R}{\partial r} = -Q_0^* \qquad 3.9$$

where Q_0^* is the flow amplitude per unit length. The equation describing flow between fracture and matrix, 3.6, becomes

$$q = -\frac{2K_f}{b}\frac{\partial Z}{\partial z} \qquad 3.10$$

The solution to these equations is

$$R = \frac{Q_0^*}{2\pi K_f} K_0(\lambda r) \qquad 3.11$$

$$\text{where } \lambda^2 = \frac{i\omega S_{sf}}{K_f}\left[1 + \frac{S_{sm}}{S_{sf}}\frac{1}{\mu b}\right] \qquad 3.12$$

$$\text{and } \mu^2 = \frac{i\omega S_{sm}}{K_m} \qquad 3.13$$

Figures 3.3 and 3.4 illustrate the variation of amplitude and phase of this solution with frequency and distance.

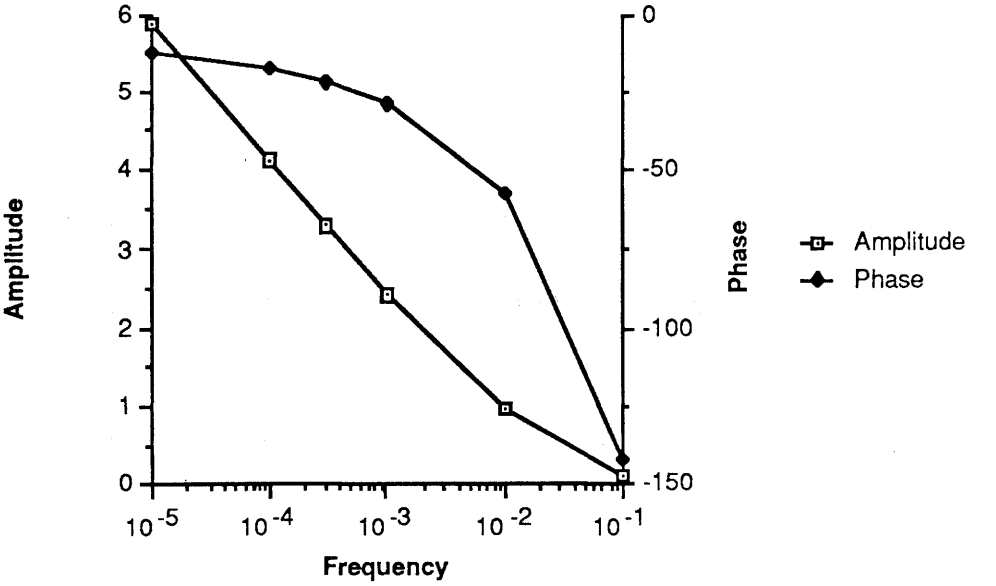

Figure 3.3 Variation of amplitude and phase shift with frequency for a two dimensional fissure flow system

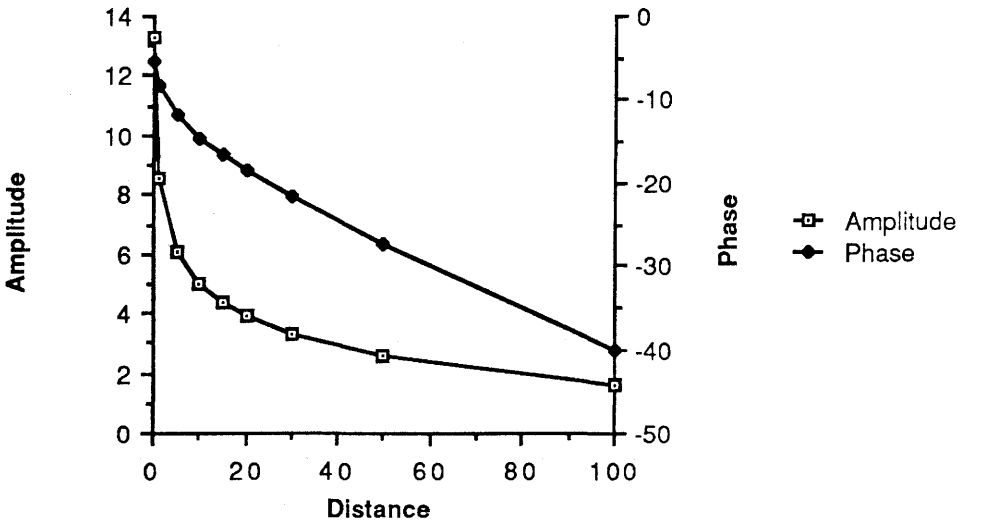

Figure 3.4 The variation of amplitude and phase shift with distance for a two dimensional fissure flow system

4. Channels (1-D)

The models described above have made use of idealized three and two dimensional flow concepts. One further simple concept, flow confined to a single cylindrical pipe, or channel, surrounded by matrix material. It will be seen that the fissure system flow in this case is one dimensional, matrix flow is radially out from the pipe and equations 3.1 and 3.2 become

$$S_{sf} \frac{\partial h_f}{\partial t} = q + K_f \frac{\partial^2 h_f}{\partial r^2} \qquad 3.14$$

$$S_{sm} \frac{\partial h_m}{\partial t} = \frac{K_m}{z} \frac{\partial}{\partial z}\left[z \frac{\partial h_m}{\partial z} \right] \qquad 3.15$$

for the fracture and matrix flow respectively. A solution of the form given in equation 3.3 is again required. The boundary conditions, for the fracture, are

$$\lim_{r \to \infty} \quad R = 0 \qquad 3.16$$

$$\lim_{r \to 0} \quad 2\pi b^2 K_f \frac{\partial R}{\partial r} = -Q_0 \qquad 3.17$$

where b is the radius of the channel. The matrix boundary conditions are

$$\lim_{z \to \infty} \quad Z = 0 \qquad 3.18$$

$$R = Z\Big|_{z=b} \qquad 3.19$$

$$q = \frac{2K_m}{b} \cdot \frac{\partial Z}{\partial z}\Big|_{z=b} \qquad 3.20$$

The solution to the flow equation 3.15, may be written

$$Z = \frac{R\ K_0(\alpha z)}{K_0(\alpha b)} \qquad 3.21$$

$$\text{where} \quad \alpha^2 = \frac{i\omega S_{sm}}{K_m} \qquad 3.22$$

Putting this in equation 3.20, we obtain

$$q = -\frac{2K_m}{b} \cdot \frac{R}{K_0(\alpha b)} \cdot \alpha K_1(\alpha b) \qquad 3.23$$

Thus the fissure flow equation becomes

$$i\omega S_{sf} R = -\frac{2\alpha R K_m}{b} \cdot \frac{K_1(\alpha b)}{K_0(\alpha b)} + K_f \frac{\partial^2 R}{\partial r^2} \qquad 3.24$$

The solution to this equation can be written as

$$R = \frac{Q_0\, e^{-\lambda r}}{2\pi b^2 \lambda K_f} \qquad 3.25$$

$$\text{where } \lambda^2 = \frac{i\omega S_{sf}}{K_f} + \frac{2\alpha R K_m}{b K_f} \cdot \frac{K_1(\alpha b)}{K_0(\alpha b)} \qquad 3.26$$

and equations 3.16 and 3.17 have been used to evaluate the coefficients. Figures 3.5 and 3.6 illustrate the variations of this solution with frequency and distance.

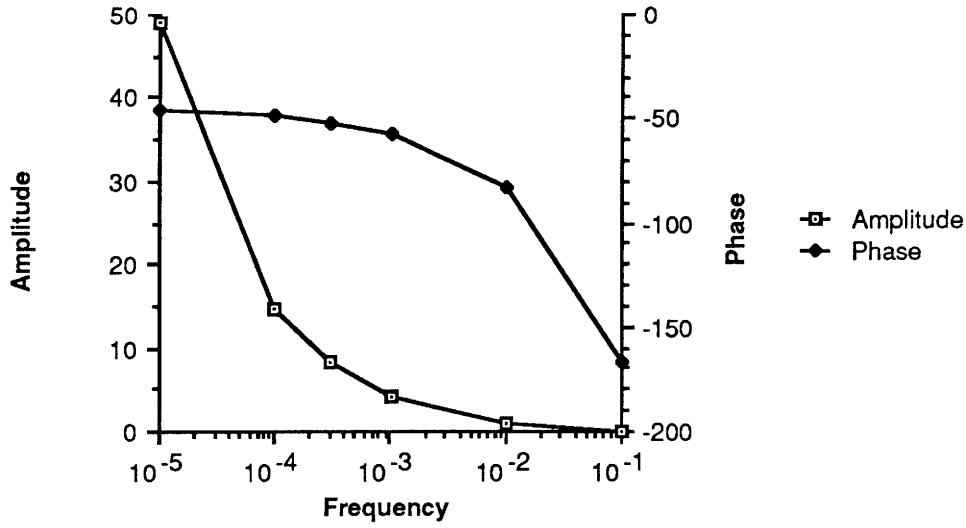

Figure 3.5 The variation of amplitude and phase shift with frequency for a one dimensional fissure flow system

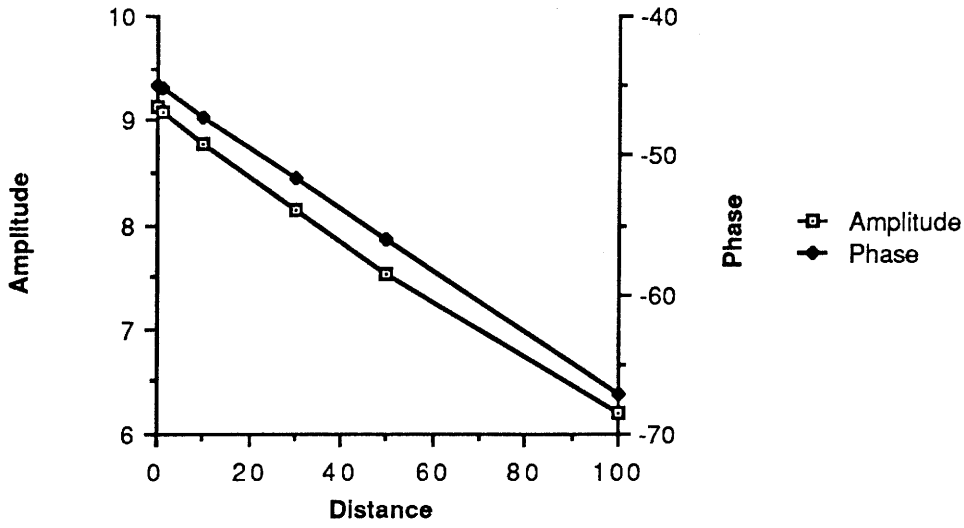

Figure 3.6 The variation of amplitude and phase shift with distance for a one dimensional fissure flow system

3.1.5 Fractional dimension fissure system

The three models described above have all assumed a specific simplified geometry for the fissures under test. In order to apply these models under realistic conditions, the properties of the matrix component have to be chosen so that they in some way reflect the presence of offshooting channels and fractures, which may themselves have a wide range of properties, in addition to the true rock matrix. Attempting to apply these models to data obtained at Stripa has proven unsatisfactory and we are lead to consider an alternative conceptualization of the fissure system flow. Instead of restricting the fissure flow to integer dimension values we suppose that fractional values may be allowed also, confined to the range 1 to 3. Within this conceptual framework the effect of offshooting channels and fractures is to increase the effective dimension of the fissure system flow. Thus as flow expands from a single channel into a fracture plane, via channel interconnections, the dimension parameter increases from 1 to 2. As flow expands away from a single plane the dimension parameter increases towards 3. The calculated value of the dimension parameter would therefore be expected to vary with the distance between source and receiver points, the functional form depending upon the statistics of the fissure system (frequency of fissure intersections, variation of fissure orientation, degree of interconnection of channels, etc.). In order to keep the development as clear as possible, the solution for fractional dimension fissure flow will be initially considered without a matrix component. This latter will be added at the end. Inspection of quations 3.1, 3.8, and 3.14 suggest that the form of the fissure flow equation should be

$$S_{sf}\frac{\partial h_f}{\partial t} = \frac{K_f}{r^{n-1}}\frac{\partial}{\partial r}\left[r^{n-1}\frac{\partial h_f}{\partial r}\right] \qquad 3.27$$

where n is the dimension parameter of the fissure flow system.(This equation is derived more rigorously in Appendix A). As before, a solution of the form of equation 3.3 is required and the boundary conditions are

$$\lim_{r \to \infty} \quad R = 0 \qquad 3.28$$

$$i\omega S_w \; R\Big|_{r=r_w} = Q_0 + K_f b^{3-n} \frac{2\pi^{n/2}}{\Gamma(n/2)} r_w^{n-1} \left.\frac{\partial R}{\partial r}\right|_{r=r_w} \qquad 3.29$$

where the point source approximation of the earlier models has been extended and the source zone has been given a finite radius, r_w, and a finite source zone storage capacity, S_w.(The derivation of equation 3.29 is also given more fully in Appendix A). Using equation 3.3, equation 3.27 becomes

$$i\omega S_{sf} R = \frac{K_f}{r^{n-1}} \frac{\partial}{\partial r}\left[r^{n-1} \frac{\partial R}{\partial r}\right] \qquad 3.30$$

The solution of equation 3.31 subject to condition 3.28 is

$$R = A r^{\nu} K_{\nu}(\lambda r) \qquad 3.31$$

$$\text{where} \quad \nu = 1 - n/2 \qquad 3.32$$

$$\text{and} \quad \lambda^2 = \frac{i\omega S_{sf}}{K_f} \qquad 3.33$$

Taking the derivative of equation 3.31, using the boundary condition, equation 3.29, and rearranging we have

$$A = \frac{Q_0}{i\omega S_w r_w^{\nu} K_{\nu}(\lambda r_w) + \dfrac{2\pi^{n/2}}{\Gamma(n/2)} K_f b^{3-n} \lambda r_w^{1-\nu} K_{\nu-1}(\lambda r_w)} \qquad 3.34$$

Putting equation 3.34 with equation 3.31 gives the required solution. This solution has been derived without the introduction of a matrix component, but it can easily be extended to include such a component by modifying

Putting equation 3.34 with equation 3.31 gives the required solution. It has been derived without a matrix component, but it can easily be extended to include such a component by modifying equation 3.33 which becomes

$$\lambda^2 = \frac{i\omega S_{sf}}{K_f} [\, 1 + \sigma B(\mu) \,] \qquad 3.35$$

where σ is the ratio of matrix to fissure storage per unit volume, B is the block geometry function, and μ is given by

$$\mu^2 = \frac{i\omega S_{sm} a^2}{K_m} \qquad 3.36$$

where a is the ratio of volume to surface area of the matrix blocks. Some details of the properties of the block geometry function have been given in Black and others, (1986), and it is discussed in depth in Barker (1985a,b).

3.2 Application of theory to responses measured at Stripa

3.2.1 Introduction

The following methodology has been adopted in attempting to interpret the data in Table 3.4. First, the "major responses" (see below) in each zone have been considered and the receiver zone signal interpreted in terms of both the 1 and 2 dimensional models described above (the 3 dimensional model was considered to be clearly inappropriate in view of the gross zonation observed). These interpretations were then tested for validity by predicting the fluctuations of head based on the applied flow regime that should have been observed in the source zone. In all cases these predictions were found to be poor. The fractional dimension model was then applied in the same way and it was found that, with suitable choice of dimension parameter, the source zone prediction could be substantially improved. The higher frequency data were then examined and it was found that, in addition to the expected dependence upon distance, the dimension parameter may also be a function of the frequency of the source zone signal.

3.2.2 Major responses in zone A

The major responses are defined to be those obtained for a particular source/receiver borehole pair with the longest period of sinusoid. When several adjacent zones in the receiver borehole respond the response with the largest amplitude is chosen. It will be seen from Table 3.4 that there are no results between boreholes 2 and 5 in this zone. Also the results for tests between boreholes 3 and 4 , and between 2 and 3 appear to be erratic so these are not considered for interpretation. Three pairs of results remain :-

Line A (4/5)

T=1440 min.	R=27 m.	Q=3.5 E-6 m^3/s.
A=0.769 m.	A_{source}=9.89 m.	
ϕ= 37 ^{o}	ϕ_{source}= 2.7 ^{o}	

Line D (2/4)

T=480 min.	R=15 m.	Q=2.0 E-6 m^3/s.
A=5.8 m.	A_{source}=9.74 m.	
ϕ= 15 o	ϕ_{source}= 9 ^{o}	

Line E (3/5)

T=720 min.	R=14 m.	Q=1.7 E-6 m^3/s.
A=1.83 m.	A_{source}= 9.66 m.	
ϕ= 51 ^{o}	ϕ_{source}= 11 ^{o}	

To interpret these results with the single fracture and channel models the matrix conductivity and specific storage were set to 1.0 E-12 m/s and 1.0 E-10 m-1 respectively. The channel dimension, b, was set to 0.01 m. Using these values in each model the fracture transmissivity and storage were determined such that equations 3.4 and 3.25 predicted the receiver zone amplitude and phase correctly. The values thus determined are termed the estimated transmissivity (T_{est}) and storage (S_{est}) for the particular model. The validity of these estimates, and of the model itself, was tested by using them to predict the amplitude and phase of the head in the source zone.The measure

of error used here is just the distance between predicted and observed points in the two dimensional result space. The results were as follows :-

Line A (4/5)		Predicted	Observed	Error
2D :-	T_{est}=8.2 E-7 m^2/s	A_{source}=4.89 m.	9.89 m.	5.02
	S_{est}=3.5 E-6	ϕ_{source}=6.27 ^{o}	2.7 ^{o}	
1D :-	T_{est}=1.66 m^2/s	A_{source}=0.93 m.		9.27
	S_{est}=4.0 E-8 m	ϕ_{source}=48.7 ^{o} * convergence failure		

It is apparent that neither model makes a satisfactory prediction of the source zone signal. The fractional-dimension model was then applied as follows. Starting from a value of 2.0, the dimension parameter was stepped in increments of 0.05. At each step, the receiver zone signal was used to estimate values for fracture conductivity and storage. These values were then used to calculate a predicted source zone response from which the error could be determined. Steps were continued until a minimum in the error was defined. For this case the minimum was found at a dimension of 2.15D and the derived results were as follows: (measured values in brackets)

K_{est}=1.88 E-5 m/s	A_{source}=8.96 m.(9.89m)	0.94
Ss_{est}=1.06 E-4 s-1.	ϕ_{source}=3.6 ^{o} (2.7^o)	

The process was repeated for the other pairs in Zone A

Line D (2/4)		Predicted	Observed	Error
2D :-	T_{est}=1.6 E-7 m^2/s	A_{source}=17.0 m.	9.74 m.	7.31
	S_{est}=1.4 E-8	ϕ_{source}= 5.06 ^{o}	9.0 ^{o}	
1D :-	T_{est}=2.8 E-3 m^3/s	A_{source}=5.8 m.		4.02
	S_{est}=2.0 E-9 m	ϕ_{source}=15.0 ^{o}		

A minimum was found at a dimension of 1.85 D with the derived results:

K_{est}=1.03 E-4 m/s	A_{source}=9.77 m (9.74)	0.05
$S_{s\ est}$=1.0 E-6 s-1.	ϕ_{source}=8.8 ^{o} (9.0^o)	

Line E (3/5)		Predicted	Observed	Error
2D :-	T_{est}=1.08 E-7 m2/s	A_{source}=15.1 m.	9.66 m.	5.49
	S_{est}=2.4 E-6	ϕ_{source}= 7.48 ^{o}	11.0 ^{o}	
1D :-	T_{est}=3.7 E-5 m^3/s	A_{source}= 2.05 m.		8.04
	S_{est}=3.2 E-5 m	ϕ_{source}= 45.0 ^{o}		

The minimum was found at a value of 1.85 D with the following derived results:

K_{est}=4.2 E-5 m/s	A_{source}=9.40 m (9.66)	0.26
$S_{s\ est}$=7.5 E-4 s-1.	ϕ_{source}=11.23 ^{o} (11.0 ^{o})	

It can be seen that the fractional-dimension model is the more successful in predicting the source zone signal given a fit to the receiver zone signal. It is also interesting to note that the two lines which indicate similar dimensionality are of similar length, whilst the longer line indicates a larger dimensionality.

The major responding zone on line A (between boreholes 4 and 5) has been measured at only one frequency, but the other two lines have been tested at two higher frequencies. It is therefore important to examine how these results relate to those obtained at the longer periods. The fits obtained above using the fractional-dimension model were used to predict both source and receiver responses at the other frequencies with the following results :-

period	source or receiver	Predicted	Observed	Error
Line D (2/4)				
40 mins	Source	A=12.16 m.	10.2 m.	7.44
		ϕ=9.4 ^{o}	47 ^{o}	
	Receiver	A= 5.85 m.	6.6 m.	3.54
		ϕ=19.7 ^{o}	52 ^{o}	
10 mins	Source	A= 23.3 m.	12.7 m.	16.30
		ϕ= 9.8 ^{o}	52 ^{o}	
	Receiver	A= 9.41 m.	6.5 m.	6.03
		ϕ= 24.5 ^{o}	64 ^{o}	

period	source or receiver	Predicted	Observed	Error
Line E (3/5)				
12mins	Source	A=5.30 m. ϕ=14.6 ^{o}	8.65 m. 8 ^{o}	3.44
	Receiver	A= 0.02 m. ϕ=111.0 ^{o}	0.23 m. 49 ^{o}	0.22
6 mins	Source	A= 3.89 m. ϕ= 15.6 ^{o}	9.43 m. 20 ^{o}	5.56
	Receiver	A= 0.003 m. ϕ= 182.3 ^{o}	0.099 m. 60 ^{o}	0.1

It is apparent that the predicitions made for both lines are rather poor and that the discrepancy increases with increasing frequency. In order to explain these higher frequency data it has been found necessary to re-interpret these lines using different values for the dimensionality. Considering line D first, a 1.2D geometry was found (by trial and error) to be appropriate with the addition of a source zone storage described by an effective radius of 2mm. (See Section 2.2.3). When the receiver zone signal for a sinusoidal test at 40 min. period is analysed assuming this geometry the estimated values of conductivity and specific storage of the fracture system are 1.8e-2 and 1.9e-3 respectively. These values can then be used to predict the other responses :-

Line D (2/4) Predictions assuming a dimensionality of 1.2 D

Period	source or receiver	Predicted	Observed	Error
40 mins	Source	A=8.59 m. ϕ=40.2 ^{o}	10.2 m. 47 ^{o}	1.96
10 mins	Source	A=10.13 m. ϕ=44.9 ^{o}	12.7 m. 52 ^{o}	2.93
10 mins	Receiver	A=6.26 m. ϕ=67.8 ^{o}	6.5 m. 64 ^{o}	0.49

Thus it would seem that the higher frequency results can be better understood if they are considered separately from the lower frequency observations. In this case the high frequency results suggest a lower dimensionality.

Considering now the results for line E, it is found that in contrast a higher value of the dimensional parameter is required. Using a 2.5 D geometry and a source zone storage of 1mm. , and interpreting the receiver zone response at a

period of 12 min. yields the parameters K_{est}=1.18e-6 m/s and $S_{s\,est}$=6. 8 E-7 s-1 for the fracture system. Predicting the other short period results with these parameters gives :-

Line E (3/5) Predictions assuming a dimensionality of 2.5 D

Period	Source or receiver	Predicted	Observed	Error
12 mins	Source	A=10.86 m. ϕ=11.2 ^{o}	8.65 m. 8 ^{o}	2.27
6 mins	Source	A=8.45 m. ϕ=20.7 ^{o}	9.43 m. 20 ^{o}	0.99
6 mins	Receiver	A=0.136 m. ϕ=71.6 ^{o}	0.10 m. 60 ^{o}	0.04

Again, it is seen that the predictions are improved by allowing short and long period observations to be interpreted using separate geometric properties.

3.2.3 Major responses in zone C

The data for zone C are sparser than for zone A, with no results for the lines between boreholes 4 and 5, 3 and 4, or 2 and 4. Further, the signal seen in borehole 5 when using borehole 2 as a source is believed to have been received via borehole 3. Finally, the longest period results for the line between boreholes 2 and 3 are probably of little value since the test lasted for less than one cycle. The major responses in this zone are therefore represented by the following two data pairs :-

Line E (3/5)

T=1440 min.	R=36 m.	Q=3.89e-6 m^3/s
A=3.05 m.	A_{source}=7.28 m.	
ϕ=36.1 ^{o}	ϕ_{source}=18.6 ^{o}	

Line F (2/3)

T=720 min.	R=31 m.	Q=1.89e-6 m^3/s
A=1.70 m.	A_{source}=9.46 m.	
ϕ=49.7 ^{o}	ϕ_{source}=12.5 ^{o}	

These results were interpreted in the same way as the zone A results, by first considering single fissure and channel models and then adopting the fractional-dimension approach. As before matrix parameters of K=1.0e-12 m/s and Ss=1.0e-10 s-1. were used and a channel size, b, of 0.01 m. The receiver zone signal was used to estimate values for the fracture system transmissivity and storage and then the source zone signal was predicted :-

Line E (3/5)		Predicted	Observed	Error
2D :-	T_{est}=2.35e-7 m^2/s	A_{source}=19.81 m.	7.28 m.	12.81
	S_{est}=5.17e-7	ϕ_{source}=5.98 ^{o}	18.6 ^{o}	
1D :-	T_{est}=0.58 m^3/s	A_{source}=3.26 m.		4.45
	S_{est}=3.58e-8 m	ϕ_{source}=41.3 ^{o}	* convergence failure	

best minimum at 1.7 D (period = 1440 mins)

	K_{est}=5.8e-4 m/s	A_{source}=7.37 m.	0.48
	$S_{s\ est}$=5.6e-4 s-1	ϕ_{source}=14.9 ^{o}	

Line F (2/3)		Predicted	Observed	Error
2D :-	T_{est}=1.32e-7 m^2/s	A_{source}=15.64 m.	9.46 m.	6.31
	S_{est}=5.5e-7	ϕ_{source}=6.56 ^{o}	12.5 ^{o}	
1D :-	T_{est}=2.7e-4 m^3/s	A_{source}=1.87 m		7.95
	S_{est}=2.6e-5 m	ϕ_{source}=45.0 ^{o}		

best minimum at 1.85 D :- (period = 720 mins)

	K_{est}=5.85e-5 m/s	A_{source}=9.17 m.	0.45
	$S_{s\ est}$=1.95e-4 s-1.	ϕ_{source}=10.4 ^{o}	

As in zone A, a significant improvement in the prediction of the source zone signal is obtained by using the fractional-dimension concept. It may be noted, however, that an important difference of structure between zones A and C may be indicated. Both lines considered in zone C are longer than 30 m. but have apparent dimensionalities of around 1.8. In contrast the 27 m. line in zone A had a 2.15D geometry , whilst the lines of only 15m. length were of a 1.85D geometry.

As shown in Table 3.4, both the lines considered here were also tested with shorter period sinusoids so the interpretaions obtained for the long period data can again be tested against short period results :-

Line E (3/5) Predictions assuming a dimensionality of 1.7D

period	source or receiver	Predicted	Observed	Error
60 mins	Source	A=10.35 m.	5.32 m.	7.20
		ϕ=15.9 ^{o}	56.5 ^{o}	
60 mins	Receiver	A=1.28 m.	0.98 m.	0.58
		ϕ=87.0 ^{o}	112.5 ^{o}	
40 mins	Source	A=18.63 (20.7) m.	5.69 (8.26) m.	14.99
		ϕ=16.0 ^{o}	59.1 (65.2) ^{o}	(16.53)
40 mins	Receiver	A=1.75(1.94) m.	0.82(1.14)m	1.21
		ϕ=100.5 ^{o}	138.2 (132.9) ^{o}	(1.15)

Line F (2/3) assuming a dimensionality of 1.85 D

period	source or receiver	Predicted	Observed	Error
240mins	Source	A= 8.69 m.	9.45 m.	1.17
		ϕ= 10.9 ^{o}	16.5 ^{o}	
240mins	Receiver	A= 0.98 m.	1.16 m.	0.26
		ϕ= 71.0 ^{o}	61 ^{o}	
60 mins	Source	A= 9.71 m.	9.90 m.	3.21
		ϕ= 11.7 ^{o}	30.5 ^{o}	
60 mins	Receiver	A= 0.39 m.	0.47 m.	0.25
		ϕ= 120.2 ^{o}	87.8 ^{o}	
15 mins	Source	A= 13.51 m.	10.76 m.	5.50
		ϕ= 12.7 ^{o}	35.5 ^{o}	
15 mins	Receiver	A= 0.08 m.	0.17 m.	0.11
		ϕ= 143.5 ^{o}	114.6 ^{o}	

As for zone A, the predictions for short period data are seen to be rather poor. Once again, the interpretations can be improved by re-interpreting the short period data with a geometry of a different dimension. For line E the receiver zone signal with 60 min. period was analysed using a geometry of 1.3 D. This gave the fracture system parameter values K_{est}=1.8e-2 m/s and $S_{s\ est}$=2.7e-2 s-1.

The resulting predictions for the other short period data are :-

Line E (3/5) Predictions assuming a dimensionality of 1.3 D

period	source or receiver	Predicted	Observed	Error
60 mins	Source	A=5.08 m.	5.32 m.	2.23
		ϕ= 31.9 ^{o}	56.5 ^{o}	
40 mins	Source	A=8.52 m.	5.69 (8.26) m.	4.32
		ϕ= 32.0 ^{o}	59.1 (65.2) ^{o}	
40 mins	Receiver	A= 1.18 (1.31) m.	0.82 (1.14) m.	0.40
		ϕ=128.4 ^{o}	138.2 (132.9) ^{o}	(0.20)

Similarly, re-interpreting the receiver zone data for line F with a period of 60 min. and using a geometry of 2.0 D and source zone storage of 2mm. suggested fracture system parameters of K_{est}=2.85e-5 m/s and $S_{s\ est}$=4.1e-5 s-1. These values result in the following predictions :-

Line F (2/3) Assuming a dimensionality of 2.0 D

period	source or receiver	Predicted	Observed	Error
60 mins	Source	A=9.18 m.	9.90 m.	3.21
		ϕ= 11.6 ^{o}	30.5 ^{o}	
15 mins	Source	A=12.9 m.	10.76 m.	3.42
		ϕ= 22.5 ^{o}	35.5 ^{o}	
15 mins	Receiver	A=0.18 m.	0.17m.	0.14
		ϕ=161.3 ^{o}	114.6 ^{o}	

The improvement in this last set of data is rather small, but overall the same pattern is seen in zone C as was found in zone A. The short period results need to be interpreted separately from those for long period tests, using different dimensionalities in general. The dimensionality may need to be either increased or decreased

4 DISCUSSION

The analysis of data presented above can only be regarded as a first attempt at applying the fractional-dimension model. Other interpretational procedures are possible and the results could be presented in alternative forms. In particular, there were some rather arbitrary choices of :

(i) the "matrix" parameters ($K_m=10^{-12}$ m s^{-1}, $S_{sm}=10^{-10}m^{-1}$).

(ii) the representative size of the fissure system in the channel model (b=1cm.) .

(iii) the source zone storage ($S_w=\pi r_c^2$, r_c=1-5mm.).

Also we have chosen, for simplicity, to ignore the tortuosity of the system. Finally, with regard to the presentation of results, we note from equations 3.31 to 3.34 that, rather than K_f and S_{sf}, we might have presented the diffusivity, (K_f / S_{sf}) , and the scaled hydraulic conductivity, $K_f(b/r_w)^{3-n}$. The results from the major responses in each zone are shown diagramatically in relation to the bore hole configuration in Figures 4.1 and 4.2. On these diagrams the diffusivities along each connection are shown.

The effective dimension of the fracture system is expected to increase both with the source-receiver separation and with sinusoidal period. The former expectation reflects the fact that over short distances flow in the local fissure system will be dominated by just a few (near one-dimensional) channels, while over very large distances the flow will be characteristic of a large number of intersecting fissures forming a (near three-dimensional) network. The reason for expecting the dimension to increase with increasing sinusoidal period is that the depth of penetration of a signal (and hence the fissure region sampled) should vary with the inverse square-root of frequency. More quantitatively, we might express a characteristic penetration depth, d_c, in the form

$$d_c^2 = 4\pi K_f / (\omega S_{sf})$$

Considerable problems arise from the variabiliy of dimension with distance and frequency. This seems to force us to analyse each test result (a phase and an amplitude) separately. Consequently, it is necessary to make assumptions about the values of all but two of the model parameters. It would be far preferable to analyse all of the data - or, at least, all of the data from a single

fissure zone - with identical or related model parameters. However, this would appear to require the assumption of a formal relationship between the flow dimension, n, and the scale, x, and the frequency, ω. Just as an example, it might be assumed that

$$n = 3 - 2\exp(-x/x_0)$$

where x_0 is a characteristic distance; or n might be related to ω by replacing x by d_c, given above.

Having introduced the concept of a fractional dimension flow system it is important to consider how this parameter (or "scale function") can be related to other concepts and models. At this early stage we can only suggest a methodology for investigating this relationship, which is simply to simulate sinusoidal tests on any given model and analyse the results using the formulae presented in this report. However, we would hope the the dimension could ultimately be related, analytically, to the characteristic parameters of other models. (Further discussion can be found in Barker (in press).)

If the results are interpreted in more physical terms then a number of aspects present themselves. It is apparent that the analyses are by no means certain but some general interpretations are perhaps possible.

There were fewer crosshole responses than would have been suggested by the core logging and the work reported from the SAC period of work (see Gale and others, 1987). This may have been a result of the limited penetration of the sinusoidal signal or it could have resulted from the extremely tight control which was exercised over spurious responses. These were often thought to travel via adjacent boreholes and this was eliminated where possible. Perhaps previous studies in fractured rock have over-estimated the degree of connection which pertains through the fracture system.

The zones A and C do not seem to respond to the testing as if they were simple planar features. Rather they respond with dimensions less than 2 suggesting that they are channellised in some way. Further they do not respond in the same way and the dimension of the zone which was tested over the larger scale (zone C) appears to respond with a smaller dimension. A physical interpretation of this would be a more sparsely channelled fracture zone. Another general observation is the trend in zone A for the diffusivity to decrease in the direction of increasing bifurcation as deduced from the qualitative interpretation. This would correspond to a single channel branching into a number of smaller channels so that the overall porosity remains constant whilst the overall conductance diminishes.

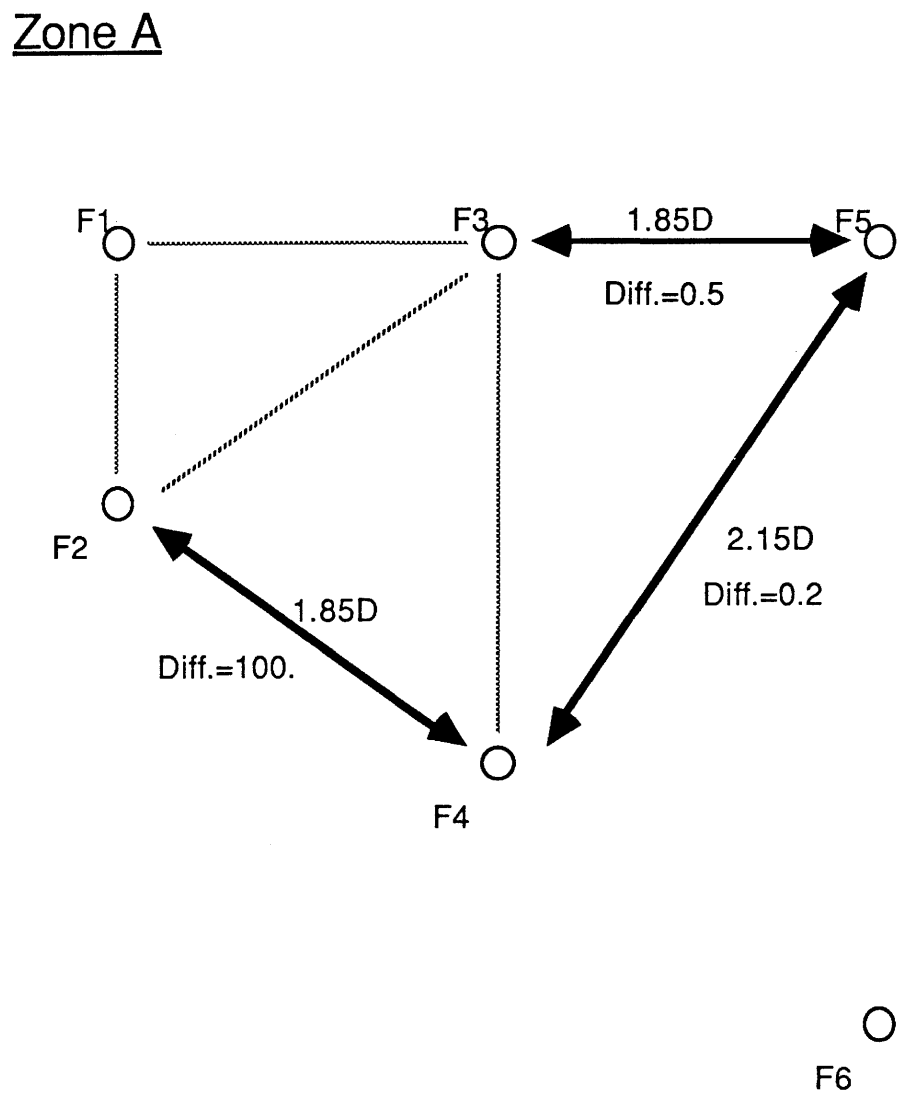

Figure 4.1 A summary of fractional dimension results shown diagramatically in relation to the borehole layout in Zone A. The diffusivity along each connection is also shown.

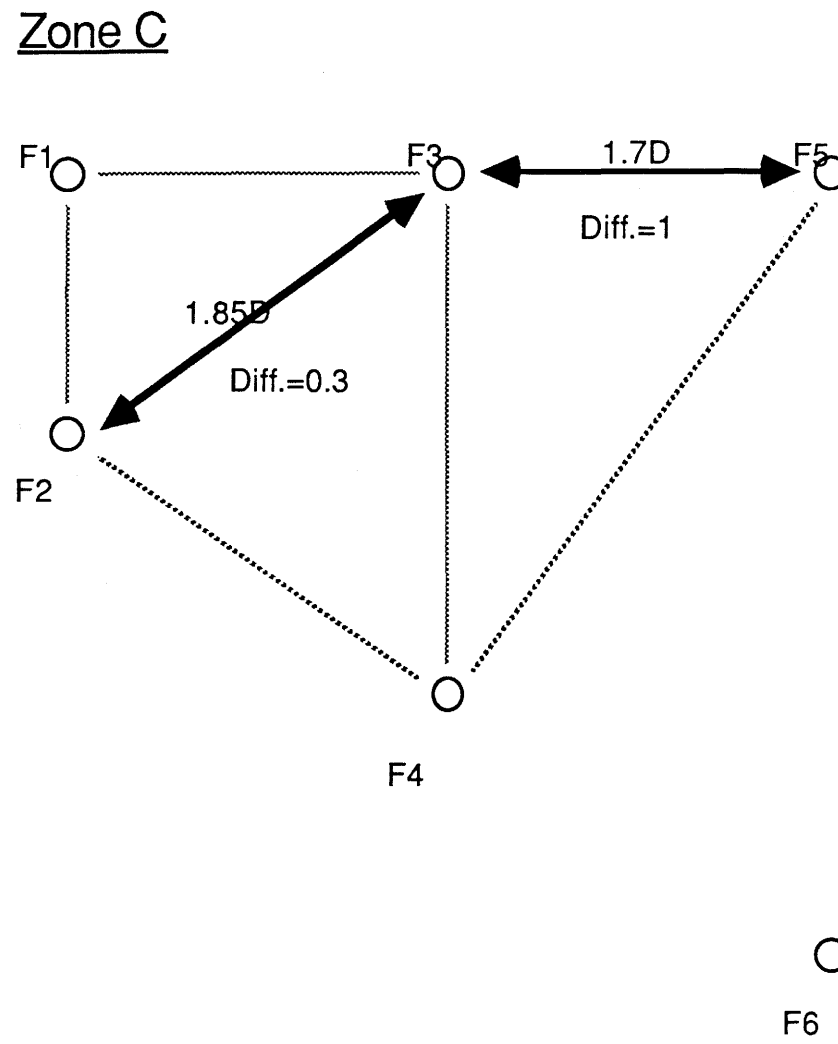

Figure 4.2 A summary of fractional dimension results shown diagramatically in relation to the borehole layout in Zone A. The diffusivity along each connection is also shown.

5. CONCLUSIONS

The hydraulics programme of the Crosshole Project had roughly two aims, to "calibrate" the geophysical methods and to evaluate sinusoidal testing. The calibration of the geophysical methods is dealt with in another report (Olsson and others, 1987). In evaluating sinusoidal testing a wide range of hydrogeological issues have been raised, ranging from straightforward technolological considerations to the fundamentals of how groundwater flow is conceived. The conclusions can therefore be divided into those concerning the technology of sinusoidal testing and those concerning the theoretical aspects.

5.1 TECHNOLOGICAL CONCLUSIONS

The programme showed that it is possible to design and construct a complex set of computer-controlled equipment and operate it regularly in the mine environment. The innovative aspects of the equipment were the use of the computer for test operation and close control of all hydraulic fluctuations in the region of the source. This resulted in good quality data with a high resolution and a close adherence to the analytical assumptions underlying the test. Some individual aspects of the equipment which were novel and worked well were:

- the use of rubber cone sealing of the boreholes during testing to reduce time involved in moving
- the use of a second pump to control the "rest-of-borehole" zone
- the use of a reference pressure system
- the use of computer-protected differential pressure transducers

The sinusoidal testing had attributes which were not expected. Firstly it proved very easy to create a sinusoidal fluctuation since it requires neither rapid changes of flow rate or head or long periods of steady conditions. The computer produced sinusoidal fluctuations which were ideal. The attributes which were expected were those concerning perception of the signal against a changing background. This proved easy in practice and results were easily adjusted for drift during the test. Another aspect was the return to equilibrium following a period of testing which ran according to expectation.

5.2 THEORETICAL ASPECTS OF SINUSOIDAL TESTING

In order to consistently interpret both source and receiver signals in these crosshole sinusoidal tests in fractured granite the concept of a fractional-dimension fracture system has been developed. This allows the treatment of channels, fissures,and homogeeously fractured rock as special cases of a continuous spectrum of flow concepts.

Results from long and short period tests need to be interpreted separately. It may be suggested that this is due to the presence of different sizes of features in the fracture system. Thus small scale features dominate the short period responses whilst larger features determine the response to longer period input signals.

Fracture system conductivities measured by long period signals in zone A range from 1.9 E-5 to 1.0 E-4 m/s., whilst in zone C values of 5.9 E-5 and 5.8 E-4 were found. The dimensionality of zone C was found to be lower at larger distances than zone A, suggesting that it might be a thinner zone or possibly just less interaction between the channels. The interpretation of the short period data from zone A between boreholes 3 and 5 in terms of a 2.5D geometry also suggests that this zone is "thick" by comparison with a 12 min. period wave in this region.

The development of the fractional dimension analysis represents a first step towards flow concepts which have a universal application. It seems possible that it represents a practical method for deriving general hydraulic properties of channelled fracture zones. These zones are the most difficult hydrogeological scale to work at because they are neither single geometrical entities nor effective equivalent porous media. This general index of response in a field test may thus provide information which can be simulated by the current range of network models.

In general it is clear that the fractional dimension approach requires further investigation. Even at this early stage it provides fresh insights into the hydraulics of fracture zones.

6. ACKNOWLEDGEMENTS

The authors would like to thank the staff of SGAB, particularly Olle Olsson, Mikhael Sehlstedt, Lars Falk and Eric Sandberg for all their help and assistance. Additionally our thanks go to Hans Carlsson, Bengt Stillborg and Gunnar Ramqvist of the Stripa Project who made our tasks easier. Finally we acknowledge the help of a large number of our B.G.S. colleagues, in particular Jean Alexander, David Noy and John Barker.

7 REFERENCES

Abelin,H., Neretnieks,I. ,Tunbrant,S. ,and Moreno,L.,(1985). Migration in a single fracture: Experimental results and evaluation, final report. Stripa Project, Stockholm, Sweden.

Abramowitz, M. and Stegun, I.A., 1964. Handbook of mathematical functions with formulas, graphs and mathematical tables. National Bureau of Standards, Washington.

Barker, J.A., 1985a. Block geometry functions characterizing transport in densely fissured media. Journal of Hydrology, 77, p263-279.

Barker, J.A., 1985b. Modelling the effects of matrix diffusion on transport in densely fissured media. Memoires 18th. Cong. of Int. Assoc. Hydrogeologists, Cambridge, June 1985. p250-269.

Barker, J.A., A generalised radial-flow model for pumping tests in fractured rock submitted to Water Resources Research

Black, J.H. and Kipp, K.L. Jr., 1977. The significance and prediction of observation well response delay in semi-confined aquifer test analysis. Groundwater, Vol. 15, pp 446 - 451.

Black, J.H. and Kipp, K.L. Jr., 1981. Determination of hydrogeological parameters using sinusoidal pressure tests: a theoretical appraisal. Water Resources Research, Vol. 17, pp. 686-692.

Black, J.H., Holmes, D.C. and Noy, D.J. 1985. Hydraulic testing in granite using the hydraulic wave method. Report of the British Geological Survey, ENPU 82 - 4, pp. 30.

Black, J.H., Barker, J.A., and Noy, D.J., 1986. Crosshole investigations - the method, theory and analysis of crosshole sinusoidal pressure tests in fissured rock. Stripa Project IR 86-03. SKB, Stockholm.

Burrel, K.H., 1974. Evaluation of the modified Bessel functions K0(z) and

K1(z) for complex arguments. Comm. ACM, 17, p524-530

Holmes, D.C., 1984. Crosshole investigations - equipment design considerations for sinusiodal pressure tests. Stripa Project IR 84-05. SKB, Stockholm.

Holmes, D. C.,and Sehlstedt, M., 1987. Crosshole investigation - Details of the construction and operation of the hydraulic testing system. Internal Report of the Stripa Project 87-04, SKB, Stockholm, 1987. 70 pages.

Olsson, O., Falk, L., Forslund, O., Lundmark, L. and Sandberg, E. 1987. Crosshole investigations - Results from borehole radar investigations. Internal Report of the Stripa Project 87 - 11 , SKB, Stockholm, 1987.

Strassen, H.H., 1975. Double precision complex Bessel function Jn(z). CERN Computer Centre Program Library, Routine C332.

Watson, G.N., 1986. Theory of Bessel functions. Cambridge University Press, London.

APPENDIX A.

A.1 Derivation of generalized radial flow equations.

The fractional dimension fissure flow model discussed in the text may be thought of as a generalization of the radial flow concept. In this appendix the equations governing such flow are derived in more detail. First, the main assumptions that must be made are listed.

a) Flow is radial, n-dimensional flow from a single source into an infinite, homogeneous and isotropic fissured medium, and is characterized by an hydraulic conductivity, K_f, and a specific storage, S_{sf}. (The extention to a dual porosity medium is discussed in the main text).

b)Darcy's law applies throughout the system.

c)The source is an n-dimensional sphere (projected through three-dimensional space - e.g. a finite cylinder when n=2) of radius r_w and storage capacity S_w (the volumetric change in storage which accompanies a unit change in head).

d) All receivers (double-packer systems with pressure transducers) have negligable size and storage capacity.

We start by considering the region bounded by two equipotentail surfaces which have radii r and r+Δr. These surfaces are the orthogonal projections of n-dimensional spheres through three dimensional space by an amount b^{3-n}. For example, when n is equal to two the surfaces are finite cylinders of length b. A sphere of radius r has an area ($\alpha_n r^{n-1}$),where α_n is the area of a

$$\alpha_n = \frac{2\pi^{(n/2)}}{\Gamma(n/2)} \qquad \text{A1}$$

unit sphere in n-dimensions:

where $\Gamma(x)$ is the gamma function. Thus the region between the equipotential shells has a volume ($b^{3-n}\ \alpha_n\ r^{n-1}\ \Delta r$) when Δr is small. Suppose that during a small period Δt the head in this shell changes by Δh, then the volume of water entering the shell must be, from the definition of specific storage, Ssf

$$\Delta V = S_{sf}\, b^{3-n}\, \alpha_n\, r^{n-1}\, \Delta r\, \Delta h \qquad \text{A2}$$

From Darcy's law, the net volumetric flow rate into the shell is

$$q = K_f b^{3-n} \alpha_n (r+\Delta r)^{n-1} \left.\frac{\partial h}{\partial r}\right|_{r+\Delta r} - K_f b^{3-n} \alpha_n r^{n-1} \left.\frac{\partial h}{\partial r}\right|_{r} \qquad A3$$

where K_f is the hydraulic conductivity and h(r,t) is the head.

The conservation equation for the water in the shell takes the form $\Delta V = q\,\Delta t$. Substituting from equations A2 and A3, and taking limits, becomes

$$S_{sf} \frac{\partial h}{\partial t} = \frac{K_f}{r^{n-1}} \frac{\partial}{\partial r}\left[r^{n-1} \frac{\partial h}{\partial r}\right] \qquad A4$$

In order to find a solution to this equation it is necessary to provide suitable boundary conditions. For the present purposes it may be assumed that the head tends to zero at large distances from the source

$$\lim_{r \to \infty} h(r,t) = 0 \qquad A5$$

The boundary condition at the source may be determined by considering the conservation of water in that region. Water is injected into the source at the rate Q(t) and flows into the region from the formation at a rate given by Darcy's law. If the storage of the source is S_w and the head is H(t), then

$$S_w \frac{\partial H}{\partial t} = Q + K_f b^{3-n} \alpha_n r_w^{n-1} \left.\frac{\partial h}{\partial r}\right|_{r=r_w} \qquad A6$$

Barker (in press) have developed solutions appropriate to more general boundary conditions (e.g. constant rate and slug tests) and have also included provision for a source zone skin effect.

APPENDIX B.

B1 COMPUTATION OF $K_\nu(z)$

A literature search failed to reveal any published algorithm for the computation of the Macdonald function, $K_\nu(z)$, of complex argument, z, and real order, ν. However, the CERN Subroutine Library (Strassen,1975) provides the routine "DBESCJ" which returns the value of the (complex) Bessel function $J_\nu(z)$. In order to obtain a reliable routine quickly, it was decided to express $K_\nu(z)$ in terms of $J_\nu(z)$, although it is recognized that a more efficient algorithm could be devised for the direct computation of the Macdonald function.

The routine "DBESCJ" returns the value of the of the function $J_c(N,\alpha,z)=J_{N+\alpha}(z)$ where N is a non-negative integer and α is a real number with the range $0\leq\alpha\leq1$. It is necessary to express $K_\nu(z)$ in terms of the function $J_c(N,\alpha,z)$. Refering to equations 5.6 and 5.8, it will be seen that we can restrict our attention to the range $-1.5\leq\nu\leq0.5$. Since $K_\nu(z)$ is symmetrical with respect to order, we need only the range $0\leq\nu\leq1.5$. Furthermore, the range of interest can be restricted to $0\leq\nu\leq1$ by using the recurrence relation

$$K_\nu(z) = K_{2-\nu}(z) + \frac{2\nu}{z} K_{\nu-1}(z) \qquad \text{B1}$$

First we note that the Macdonald function is defined in terms of the modified Bessel function of the first kind, $I_\nu(z)$

$$K_\nu(z) = \frac{(\pi/2)\,[\,I_{-\nu}(z) - I_\nu(z)\,]}{\sin(\nu\pi)} \qquad (\nu \neq \text{integer}) \qquad \text{B2}$$

Now $I_{-\nu}(z)$ can be written in terms of Bessel functions of order greater than zero by means of the recurrence relation

$$I_{-\nu}(z) = I_{2-\nu}(z) + 2\frac{(1-\nu)}{z} I_{1-\nu}(z) \qquad \text{B3}$$

Putting equation B2 in equation B1, and setting $\alpha=1-\nu$, gives

$$K_\nu(z) = \frac{(\pi/2)\left[\, I_{1+\alpha}(z) + \frac{2\alpha}{z} I_\alpha(z) - I_\nu(z)\,\right]}{\sin(\nu\pi)} \qquad \text{B4}$$

Now, the modified Bessel function of the first kind can be written in terms of the function $J_\nu(z)$

$$I_\nu(z) = \begin{cases} e^{-(\nu\pi/2)i}\, J_\nu\left(ze^{(\pi/2)i}\right) & \text{when } -\pi \le \arg z \le \pi/2 \\ e^{(3\nu\pi/2)i}\, J_\nu\left(ze^{-(3\pi/2)i}\right) & \text{when } \pi/2 \le \arg z \le \pi \end{cases} \qquad \text{B5}$$

Putting this relationship into equation B3 gives

$$K_\nu(z) = \frac{(\pi/2)\left[\Theta^{1+\alpha} J_c(1,\alpha,\zeta) + 2\frac{\alpha\Theta^\alpha}{z} J_c(0,\alpha,\zeta) - \Theta^\nu J_c(0,\nu,\zeta)\right]}{\sin(\nu\pi)} \qquad \text{B6}$$

where

$$\Theta = e^\beta \qquad \text{B7}$$

$$\zeta = \Theta z \qquad \text{B8}$$

and

$$\beta = \begin{cases} -\pi/2 & \text{when } -\pi \le \arg z \le \pi/2 \\ 3\pi/2 & \text{when } \pi/2 \le \arg z \le \pi \end{cases} \qquad \text{B9}$$

Equation B5 provides the required relationships between the Macdonald function and the CERN library function "DBESCJ" provided that we use the absolute value of the order. However, because of the restriction that equation B1 only applies to non-integral orders, we must employ an approximation for ν=0 or 1. In fact we cannot in practice use equation B5 even for values of ν which are close to zero or one because both the numerator and the denominator will become zero close to integer values of ν due to rounding errors.

Consider the expansion of $K_\nu(z)$ with respect to ν, about $\nu=0$. Since

$$\lim_{\nu \to 0} \frac{\partial K_\nu(z)}{\partial \nu} = 0 \qquad \text{B10}$$

we can write

$$K_\nu(z) = K_0(z) + k(z)\,\nu^2 + \ldots \qquad \text{B11}$$

where k is a function of z only. In particular, for $\nu=\varepsilon$ and $\nu=2\varepsilon$, we have

$$K_\varepsilon(z) = K_0(z) + k(z)\,\varepsilon^2 + \ldots \qquad \text{B12}$$

$$K_{2\varepsilon}(z) = K_0(z) + 4k(z)\,\varepsilon^2 + \ldots \qquad \text{B13}$$

Ignoring terms of order greater than ε^2, equations B11 and B12 can be solved for $K_0(z)$ and k(z), and the results substituted back into equation B10, to give

$$K_\nu(z) = \left[(4-\eta)\,K_\varepsilon(z) - (1-\eta)\,K_{2\varepsilon}(z) \right] / 3 \qquad \text{B14}$$

where $\eta = (\nu / \varepsilon)^2$. Using equation B13 with a suitably small value of ε, we can extrapolate to very small values of ν (including $\nu = 0$). A Fortran function "KNUZ", developed from B5 and B13 has been tested using the equation

$$K_{1/2}(z) = \left[\frac{\pi}{2z}\right]^{1/2} e^{-z} \qquad \text{B15}$$

for $\nu = 0.5$, and against the routine given by Burrel (1974) for $\nu = 0$. A value of 0.02 was chosen for ε after some experimentation. This and related routines are still under developement and error bounds have not been fully established.

APPENDIX C

NOTATION

a	volume to area ratio for a matrix block.
b	fissure system size parameter.
B	block geometry function.
h_f	piezometric head in the fissure system.
h_m	piezometric head in the matrix.
$I_\nu(z)$	modified Bessel function.
J_c	function implemented in CERN subroutine "DBESCJ".
$J_\nu(z)$	Bessel function.
k	coefficient of ν^2 in expansion of $K_\nu(z)$.
K_f	hydraulic conductivity of the fissure system.
K_m	hydraulic conductivity of the matrix material.
$K_\nu(z)$	Macdonald's function.
n	dimension parameter for the fissure flow system.
q	volumetric flow rate of water.
Q_0	amplitude of injection rate into the source zone.
r	radial distance from the origin (centre of the source).
r_w	radius of the source.
R	solution to fissure flow equations.
S_{sf}	specific storage of the fissure system.
S_{sm}	specific storage of the matrix material.
S_w	storage capacity of the source zone.
t	time.
V	a volume of water.
z	the distance into the matrix material a complex number.
Z	solution to matrix flow equations.
α	a parameter in the solution for channelled flow (equation 4.9) = ν - int(ν) (Appendix B).
α_n	area of a unit sphere in n dimensions.
β	a phase angle which depends upon arg(z) (Appendix B).
Γ	the gamma function.
Δ	prefix indicating a small change in a parameter.
ε	the (small) order of a Bessel function.
ζ	$= \Theta z$.
η	$= (\nu / \varepsilon)^2$.
Θ	$= e^{\beta}$.
λ	a parameter in the solution of the fissure flow equations.
μ	argument of the block geometry function.

ν = 1 - n/2.

σ ratio of the matrix storage to the fissure storage per unit volume.

ω angular frequency of a sinusoidal test.